Rapid #: -14763095

CROSS REF ID: **455146**

LENDER: **OPEN :: nature10212017**

BORROWER: **UUS :: Main Library**

TYPE:	Article CC:CCL
JOURNAL TITLE:	Mathematical medicine and biology
USER JOURNAL TITLE:	Mathematical Medicine and Biology
ARTICLE TITLE:	A reinforced random walk model of tumour angiogenesis and anti-angiogenic strategies
ARTICLE AUTHOR:	Plank, M. J.
VOLUME:	20
ISSUE:	2
MONTH:	
YEAR:	2003
PAGES:	135-181
ISSN:	1477-8599
OCLC #:	

Processed by RapidX: 5/23/2019 3:47:32 PM

Mathematical Medicine and Biology (2003) **20**, 135–181

A reinforced random walk model of tumour angiogenesis and anti-angiogenic strategies

M. J. PLANK AND B. D. SLEEMAN
School of Mathematics, University of Leeds, Leeds, LS2 9JT, UK

[Received on 23 October 2002; revised on 10 April 2003]

It is now well accepted that the growth of a tumour beyond approximately 2 mm in diameter is dependent on its ability to induce the growth of new blood vessels, a process called angiogenesis. This has raised hope that an anti-angiogenic treatment may be effective in the fight against cancer. Here we formulate, using the theory of reinforced random walks, an individual cell-based mathematical model of tumour angiogenesis in response to a diffusible angiogenic factor. The early stages of angiogenesis, in which endothelial cells (EC) escape the parent vessel and invade the extra-cellular matrix, are included in the model, as are the action of a proteolytic enzyme, EC proliferation and capillary branching and anastomosis. The anti-angiogenic potential of angiostatin, a known inhibitor of angiogenesis, is also examined. The capillary networks predicted by the model are in qualitative agreement with experimental observations. Proteolysis and proliferation are shown to be crucial for vascularization, whilst angiostatin is seen to be capable of limiting capillary growth.

Keywords: angiogenesis; angiostatin, chemotaxis; haptotaxis; reinforced random walk; tumour.

1. Introduction

Most primary solid tumours initiate as avascular clusters of cells (Folkman, 1974). Such a tumour must obtain the nutrients it needs by diffusion from a nearby capillary. The amount of nutrient that can be obtained in this way is limited and does not allow the tumour to grow beyond a certain size (typically about 1–2 mm in diameter) (Folkman, 1971). At this limiting size, the tumour is in a steady state, with cell proliferation balanced by cell death, and it may persist in this dormant phase for months or even years, without causing significant damage to the host (Carmeliet & Jain, 2000).

In order to grow further and to form metastases in distant organs, the tumour must obtain a blood supply. In many cases, this occurs by angiogenesis, the formation of new blood vessels from the existing vasculature (Paweletz & Kneirim, 1989). Angiogenesis takes place physiologically during embryogenesis (Risau, 1997), during placental growth and in the female reproductive system (Reynolds *et al.*, 1992). Angiogenesis can also be induced under pathological conditions, such as wound healing (Hunt *et al.*, 1984), rheumatoid arthritis (Carmeliet & Jain, 2000) and solid tumour growth (Folkman, 1971).

In the case of many solid tumours, angiogenesis never really stops. The tumour vasculature is constantly being remodelled, regressing in some areas and spreading in others (Vajkoczy *et al.*, 2002). If metastases form, angiogenesis will be induced at remote

sites and the rapid malignant growth it permits will, unless the cancer is successfully treated, ultimately prove fatal. So it is with the aim of modelling the process that we present a description of tumour angiogenesis.

Central to the process of angiogenesis are the endothelial cells (EC) which line all blood vessels in the body. In mature, quiescent capillaries, the EC form a single layer of flattened cells around the lumen. Cell–cell connections are tight and cell proliferation is rare (Han & Liu, 1999). The endothelium is surrounded by the basement membrane, an extra-cellular layer which serves as a scaffold on which the EC rest (Paweletz & Kneirim, 1989) (Fig. 1(a)). Peri-endothelial support cells, such as smooth muscle cells and macrophages, are also found close to the capillary.

Tumours are known to secrete various chemicals, which diffuse into the surrounding tissue, some of which are tumour angiogenesis factors, or TAFs (Folkman & Klagsbrun, 1987). The best characterized angiogenic factor is vascular endothelial growth factor (VEGF) (Leung *et al.*, 1989; Yancopoulos *et al.*, 2000), which is largely specific for EC (Shweiki *et al.*, 1992) and has been shown to be a potent chemoattractant and mitogen (Klagsbrun & D'Amore, 1996; Han & Liu, 1999). During the dormant phase, the effects of these chemicals are outweighed by growth inhibitors, some of which may be present under normal physiological conditions, some of which may be produced by the immune system in response to the tumour, and some of which may be secreted by the tumour itself (Pepper, 1997; Carmeliet & Jain, 2000). However, at some point in time, the growth factors secreted by the tumour may finally overcome the growth inhibitors, and an angiogenic response is induced in the host (Hanahan & Folkman, 1996). The switch that triggers this emergence from dormancy into activity is still the subject for research, for example see Semenza (2000) and Giordano & Johnson (2001). Many factors are involved and hypoxia (oxygen deficiency), which is known to up-regulate VEGF production (Shweiki *et al.*, 1992), is thought to have a major influence.

On receiving a VEGF stimulus, EC in capillaries near the tumour begin to loosen contacts with adjacent cells and secrete proteolytic enzymes, which degrade the basement membrane (Pepper, 1997) (Fig. 1(b)). EC subsequently move through the gap in the basement membrane and into the extra-cellular matrix (ECM), a process known as extravasation. They continue to secrete proteolytic enzymes, which also degrade the ECM (Pepper *et al.*, 1990). This allows them to migrate towards the tumour (Ausprunk & Folkman, 1977), thus forming sprouts from the parent capillary (Liotta *et al.*, 1991) (Fig. 1(c)). The migration is thought to be controlled by chemotaxis (directed cell movement up a gradient of a diffusible substance, typically a growth factor emitted by the tumour) and haptotaxis (movement along an adhesive gradient, of fibronectin for example) (Carter, 1965).

In normal endothelia, the turnover for EC is very slow, typically measured in months or years (Han & Liu, 1999). Nevertheless, a short distance behind the sprout tips, rapid EC proliferation in response to VEGF is observed, increasing the rate of sprout formation (Ausprunk & Folkman, 1977; Denekamp & Hobson, 1982).

Sprouts are seen to branch and loop (anastomose) and the beginnings of an extended vascular network are created, which gradually extends towards the tumour (Folkman & Klagsbrun, 1987). This branching and looping may become much more pronounced in the vicinity of the tumour, producing what is termed the brush-border effect (Muthukkaruppan *et al.*, 1982). Sprouts may eventually penetrate the tumour, providing it with the nutrients

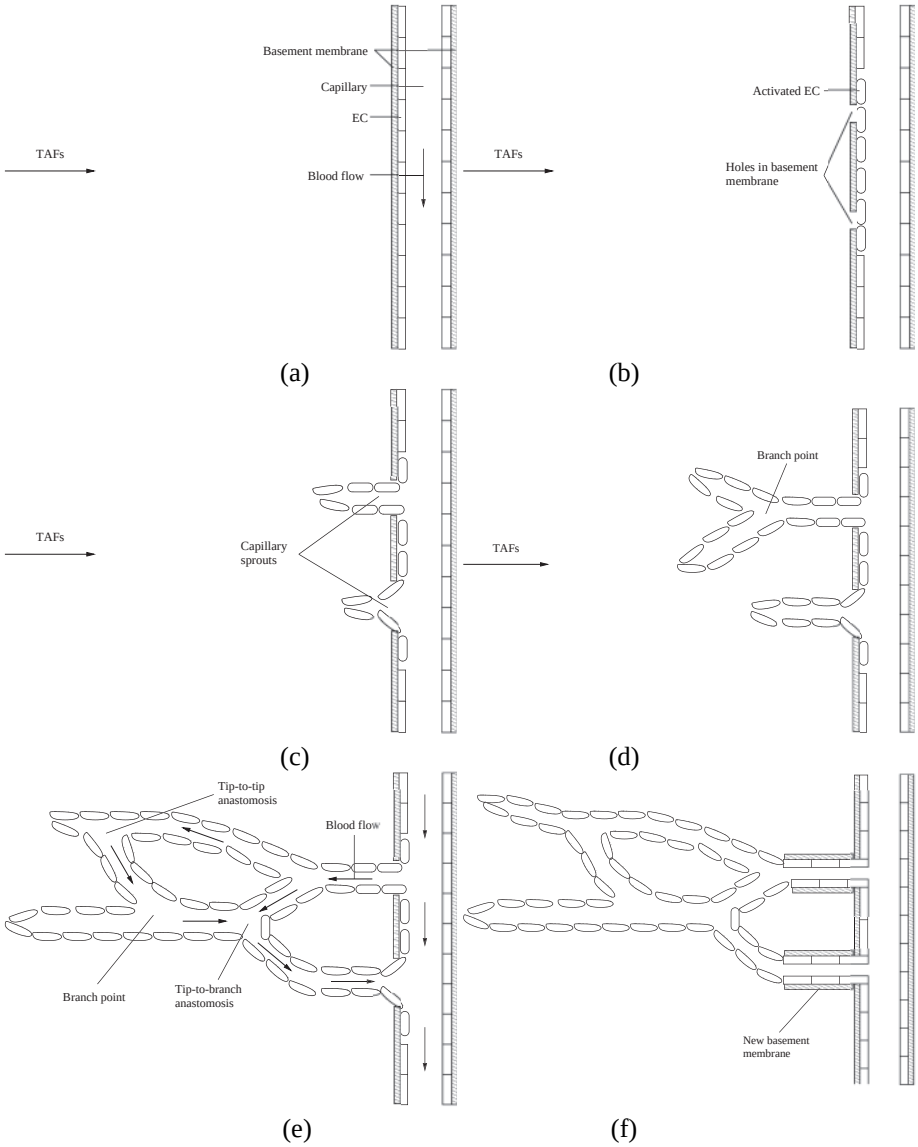

FIG. 1. The key events of angiogenesis: (a) A quiescent capillary receives TAFs secreted by a nearby tumour. (b) The EC produce protease, which degrades the basement membrane. (c) EC move out of the parent vessel, forming new capillary sprouts. (d) EC proliferation begins and capillary branching is observed. (e) Anastomosis creates closed loops and circulation can begin in the new capillaries. (f) The new vessels start to undergo maturation, involving deactivation of the EC and formation of a new basement membrane.

it needs for rapid growth. Once the tumour has established a blood supply, metastatic tumour cells can more easily enter the circulation and hence gain access to distant sites (Schirrmacher, 1985).

In normal angiogenesis, the newly formed vessels undergo a maturation process, during which a continuous endothelium and basement membrane are formed (Fig. 1(f)). However, the capillaries that grow in response to a tumour do not usually form mature, stable vessels with a continuous basement membrane and normal blood supply. Rather the new vasculature is irregular, leaky and tortuous (Hashizume *et al.*, 2000) and is constantly being remodelled as some sprouts regress and some vessels produce new sprouts (Vajkoczy *et al.*, 2002).

One of the more promising anti-angiogenic molecules is angiostatin. O'Reilly *et al.* (1994) initially discovered angiostatin, an inhibitor of EC proliferation, during an attempt to understand the observation that surgical removal of a primary tumour is often followed by the rapid growth of previously dormant and undetectable metastases. The hypothesis was that production by the primary tumour of pro-angiogenic factors locally outweighed production of angiogenic inhibitors, angiostatin in particular, resulting in the angiogenic response required by the tumour. The longer half-life of angiostatin, however, allowed it to circulate and reach the vascular bed of a metastasis in excess of angiogenic stimulators and thus inhibit secondary tumour growth. Removal of the primary tumour cuts off the source of angiostatin and angiogenesis at secondary tumours can proceed unchecked, leading to rapid growth.

Subsequent research has established that angiostatin is generated by proteolysis of plasminogen (Gately *et al.*, 1996, 1997) and that it can induce EC apoptosis (programmed cell death) and inhibit EC migration and tube formation (Claesson-Welsh *et al.*, 1998; Lucas *et al.*, 1998) as well as proliferation. Stack *et al.* (1999) hypothesized that the mechanism by which angiostatin reduces the invasive capacity of EC (and cancer cells) is via inhibition of protease production. This would also explain the inhibition of EC tube formation, whilst the induction of apoptosis could account for the observed reduction in EC proliferation (Soff, 2000).

Angiostatin thus acts both by blocking the stimulatory effects of pro-angiogenic factors (Moser *et al.*, 2002) and by direct negative effects on EC survival (Cavallaro & Christofori, 2000). Angiostatin has been shown to inhibit tumour growth in a variety of cancers (Kirsch *et al.*, 2000) and is currently undergoing clinical trials as a potential anti-cancer therapy (Cao, 2001; Burke & DeNardo, 2001).

Mathematical modelling of cell behaviour can be divided broadly into two categories: continuum models at the cell density level; and discrete models at the level of the individual cell. Models of the continuum type are usually derived from mass conservation equations and chemical kinetics. This results in a system of partial differential equations, modelling macroscopic quantities such as cell density and chemical concentrations. Examples include Balding & McElwain (1985), Chaplain & Stuart (1993) and Chaplain *et al.* (1995).

Discrete models, on the other hand, often contain a stochastic element and model at the level of the individual cell. They attempt to capture microscopic properties of the capillary network, such as sprout branching and looping, by keeping track of the movements of each individual cell. There are many different types of discrete model, such as Stokes & Lauffenburger (1991), Firmani *et al.* (1999) and Turner & Sherratt (2002). Anderson *et al.* (1997) derived a discrete model for nematode movement via a discretization of the governing continuous equation. This method has subsequently been used to generate discrete models of EC movement in angiogenesis (Anderson & Chaplain, 1998) and of tumour cell invasion (Anderson & Chaplain, 2000).

The approach taken here differs in that the master equation governing cell movement is derived directly from the governing biology, via the theory of reinforced random walks (Davis, 1990), rather than from a discretization of a continuous equation. We believe the framework of reinforced random walks developed by Othmer & Stevens (1997) is ideal for understanding the link between continuum and discrete models: see, for example, Levine *et al.* (2000, 2001b) and Sleeman & Wallis (2002).

Levine *et al.* (2001a) presented a continuum model of angiogenesis based closely on the biochemical processes involved. The model is comprised of two coupled systems: a one-dimensional system, representing a capillary, and a two-dimensional system, representing the ECM which separates the capillary from the tumour. In the capillary, the EC respond to a VEGF stimulus by producing protease, which degrades the basement membrane and eventually allows the EC to move into the ECM. Once in the ECM, the cells can migrate towards the tumour, continuing to secrete protease and thus degrading the ECM as they do so. The protease is viewed as a chemoattractant, whilst haptotaxis is assumed to have the effect of attracting the EC to areas where the density of the ECM is low. In line with experimental observations, EC proliferation is included once the cells are in the ECM. The capillary and the ECM are coupled via appropriate transmission conditions. The model thus incorporates the initial stages of angiogenesis, in which the EC must abandon their normally quiescent state and move out of the parent capillary, a feature often neglected in other models.

The effects of angiostatin, an angiogenic inhibitor, are also examined. Angiostatin is assumed to function by deactivating the protease produced by the EC (Stack *et al.*, 1999), either directly or indirectly via an intermediate, EC-derived inhibitor complex.

Here, we formulate this scenario as a discrete model, in which cell movement is viewed as a reinforced random walk (Davis, 1990; Othmer & Stevens, 1997). In Section 2, we describe the details of the mathematical model, which describes how the substrate concentrations evolve in space and time, how the EC move and how the capillary and ECM are coupled. In Section 3, the method of simulation is described, including details of how cell movement, proliferation and death take place and how these affect the observable formation of new capillaries. Finally, in Section 4, the results are presented and discussed.

2. The mathematical model

The model is constructed on the domain shown in Fig. 2 and on the time domain, $[0, T]$. The capillary is assumed to be of infinitesimal thickness, and is located on the subset of the x-axis, $[0, L]$. The ECM separating the capillary and the tumour is viewed as the rectangular subset of the x–y plane, $[0, L] \times [0, l]$. Functions defined on the capillary will be denoted by lower-case letters, $g : [0, L] \times [0, T] \to R$ whereas functions defined on the ECM will be denoted by upper-case letters, $G : [0, L] \times [0, l] \times [0, T] \to R$. We distinguish between quantities in the capillary and quantities that are just outside the capillary: in general, $g(x, t) \neq G(x, 0, t)$.

We begin with a number of EC in the capillary and a source of VEGF at the tumour. The ECM and the basement membrane are assumed to be composed of fibronectin, a principal extra-cellular component. Thus fibronectin concentration is viewed as representing the thickness of the basement membrane in the capillary and density of the ECM. The VEGF diffuses through the ECM and into the capillary, where it binds to receptors on the surface

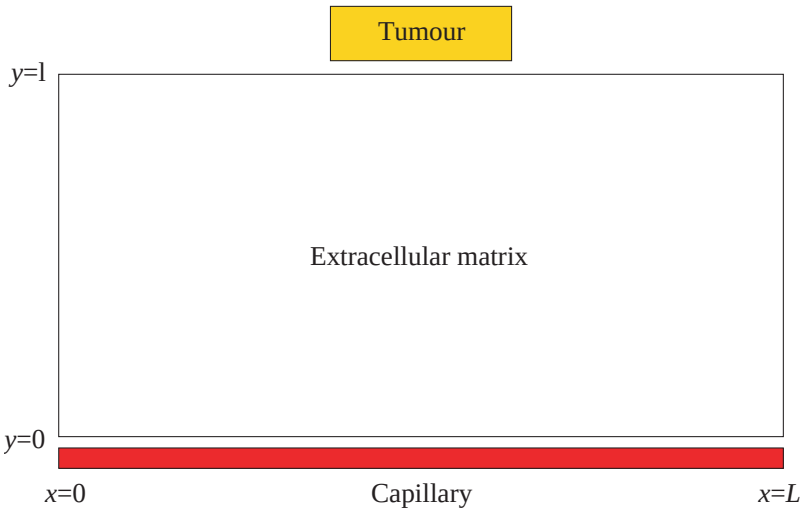

FIG. 2. Diagram of the model geometry.

of EC. This stimulates the EC to produce a proteolytic enzyme, or protease, which in turn degrades the fibronectin levels in the capillary. A Michaelis–Menten approach is used for these biochemical reactions.

When the fibronectin falls below a certain threshold level, the basement membrane has been sufficiently degraded to allow EC to escape into the ECM. The EC continue to produce protease in the ECM and can thus degrade fibronectin levels there. EC movement is governed by both random diffusion and by chemotactic and haptotactic terms. We assume, as discussed in Section 2.2, that VEGF and protease are chemoattractants for the EC, whilst haptotaxis has the effect of attracting cells to regions of low fibronectin concentration. EC proliferation in the ECM is comprised of a background growth term and a protease-dependent term, so the amount of protease produced by the EC in turn affects the EC proliferation response. A death term is also included, representing apoptosis, or programmed cell death (Liu *et al.*, 2000). We expect the EC to form sprouts from the capillary and migrate across the ECM towards the tumour.

Angiostatin, an anti-angiogenic factor, is assumed to function by directly inhibiting the actions of the protease. We will investigate whether this mechanism can curtail angiogenic activity.

2.1 *The substrate equations*

As in Levine *et al.* (2001b), we take the view that the binding of ligand to cell receptors can be modelled as an enzymatic biochemical reaction (see also Kendall *et al.* (1999)). The reaction of particular interest here is the binding of VEGF to receptors located on EC. A molecule of VEGF (V) binds to a receptor on the surface of an EC (R_V), forming a receptor–ligand complex ($R_V V$). The complex is internalized and triggers an intracellular sequence of transcription events, the result of which is the secretion of a number of

molecules of protease (C). The complex decomposes into a modified receptor (R'_V), which is subsequently recycled back to the cell surface to become R_V, where it may repeat the process. There is hence an uptake of VEGF by EC (Lai *et al.*, 1989), stimulating expression of protease (Papetti & Herman, 2002).

The transduction cascade triggered by the binding of VEGF is highly complex and involves G-proteins, amplification events and mRNA (Levine *et al.*, 2003). The process is not fully understood and many of the individual rate constants are unknown. Here we consider a simplified mechanism, which does not take account of intracellular events, but retains the most important biochemical features. This may be written symbolically as follows:

$$V + R_V \underset{k_{-1}}{\overset{k_1}{\rightleftharpoons}} R_V V$$

$$R_V V \xrightarrow{k_2} C + R_V \cdot$$

Denoting the concentration of a substance X by $[X]$, we wish to apply to this process the law of mass action, which states that the reaction rate is proportional to the product of the concentrations of the reactants. Let $[R_T]$ be the total receptor concentration (free receptors plus receptors forming the intermediate complex). In addition to the changes in the concentrations of the individual species resulting from the above reaction, $[R_T]$ may change with time due to, for example, local crowding or dispersion of cells. Taking this into account, we therefore have the following set of equations:

$$\frac{\partial [R_V]}{\partial t} = -k_1 [R_V][V] + (k_{-1} + k_2)[R_V V] + \frac{\partial [R_T]}{\partial t} \tag{1}$$

$$\frac{\partial [V]}{\partial t} = -k_1 [R_V][V] + k_{-1}[R_V V] \tag{2}$$

$$\frac{\partial [R_V V]}{\partial t} = k_1 [R_V][V] - (k_{-1} + k_2)[R_V V] \tag{3}$$

$$\frac{\partial [C]}{\partial t} = k_2 [R_V V]. \tag{4}$$

Assuming that $[R_V V](0) = [C](0) = 0$ (i.e. there is initially no protease and no receptor–ligand complex), then it follows from (1)–(4) that

$$[R_V] + [R_V V] = [R_T]$$

$$[V] + [R_V V] + [C] = [V](0),$$

where $[R_T](0) = [R_V](0)$.

We apply the Michaelis–Menten hypothesis, which says that, after a short initial transient, the concentration of the intermediate complex, $R_V V$, is in steady state

(see Murray, 1993, Chapter 5, or Schnell & Mendoza, 1997). Hence, setting $\frac{\partial [R_V V]}{\partial t} = 0$ in (3) and eliminating $[R_V]$, we deduce that

$$[R_V V] = \frac{\nu_1 [V][R_T]}{1 + \nu_1 [V]},$$

where $\nu_1 = \frac{k_1}{k_{-1}+k_2}$.

Substituting into (2) and (4), we obtain

$$\frac{\partial [V]}{\partial t} = -\frac{\lambda_1 [V][R_T]}{1 + \nu_1 [V]}$$
$$\frac{\partial [C]}{\partial t} = \frac{\lambda_1 [V][R_T]}{1 + \nu_1 [V]},$$

where $\lambda_1 = \nu_1 k_2$.

As argued in Levine *et al.* (2001b), if we assume that the total number of receptors per cell is constant (say δ_e), then we may replace $[R_T]$ by $\delta_e [EC]$, where $[EC]$ is the endothelial cell density. This gives the following rate laws:

$$\frac{\partial [V]}{\partial t} = -\frac{\lambda_1 \delta_e [V][EC]}{1 + \nu_1 [V]} \tag{5}$$
$$\frac{\partial [C]}{\partial t} = \frac{\lambda_1 \delta_e [V][EC]}{1 + \nu_1 [V]}. \tag{6}$$

The dynamics for $[EC]$ will be considered in Section 2.2.

Degradation of fibronectin (F) by protease can also be viewed as an enzymatic reaction. In addition, angiostatin acts by inhibiting the protease (Stack *et al.*, 1999). We therefore assume that the total protease (C) consists of a proportion that is active (C_A), a proportion that is inactive (C_I), as well as a proportion that is in the intermediate complex ($C_A F$). Angiostatin (A) combines with active protease to form inactive protease, which is inhibited from functioning in the degradation of fibronectin:

$$C_A + F \underset{k_{-5}}{\overset{k_5}{\rightleftharpoons}} C_A F$$
$$C_A F \xrightarrow{k_6} C_A + F'$$
$$A + C_A \underset{k_{-7}}{\overset{k_7}{\rightleftharpoons}} C_I,$$

where F' represents proteolytic fragments of fibronectin.

Again, in addition to the changes in the individual species concentrations caused by these reactions, the total protease concentration will change with time. The protease secreted by the cells is initially in the active form and so (6) provides a contribution to $\frac{\partial [C_A]}{\partial t}$†. Hence the law of mass action yields the following set of equations:

†*In vivo*, there may be additional contributions from other sources. For example, tissue plasminogen activators, which may be expressed by activated EC and by tumour cells (Pepper, 2001), convert the inert substance plasminogen into plasmin, which is a proteolytic enzyme.

$$\frac{\partial [C_A]}{\partial t} = -k_5 [C_A][F] + (k_{-5} + k_6)[C_A F] - k_7 [C_A][A] + k_{-7}[C_I] + \frac{\partial [C]}{\partial t}$$

$$\frac{\partial [F]}{\partial t} = -k_5 [C_A][F] + k_{-5}[C_A F]$$

$$\frac{\partial [C_A F]}{\partial t} = k_5 [C_A][F] - (k_{-5} + k_6)[C_A F]$$

$$\frac{\partial [F']}{\partial t} = k_6 [C_A F]$$

$$\frac{\partial [A]}{\partial t} = -k_7 [C_A][A] + k_{-7}[C_I]$$

$$\frac{\partial [C_I]}{\partial t} = k_7 [C_A][A] - k_{-7}[C_I].$$

If $[C_A F](0) = [C_I](0) = [F'](0) = 0$, then it follows that

$$[C_A] + [C_A F] + [C_I] = [C]$$

$$[F] + [C_A F] + [F'] = [F](0).$$

Assuming that the angiostatin reaction is in equilibrium, we have $[C_I] = \nu_e [C_A][A]$ (where $\nu_e = \frac{k_7}{k_{-7}}$) and hence

$$[C_A] = \frac{[C] - [C_A F]}{1 + \nu_e [A]}.$$

A similar application of the Michaelis–Menten hypothesis determines $[C_A F]$ and leads to the rate law for fibronectin,

$$\frac{\partial [F]}{\partial t} = -\lambda_3 [C_A][F]$$

where

$$[C_A] = \frac{[C]}{1 + \nu_e [A] + \nu_3 [F]}$$

and $\nu_3 = \frac{k_5}{k_{-5}+k_6}$, $\lambda_3 = \nu_3 k_6$.

Now let $v(x,t)$, $c(x,t)$, $f(x,t)$ and $a(x,t)$ respectively denote the concentrations of VEGF, (total) protease, fibronectin and angiostatin in the capillary. Also let $p(x,t)$ denote the EC density. Combining the reaction kinetics described above with

- a source term, $v_r(x,t)$, allowing VEGF to pass into the capillary from the ECM.

- natural decay of protease (with rate constant $\mu \geqslant 0$).
- logistic production of fibronectin by the EC (with carrying capacity f_0)†.
- a source of angiostatin, $a_r(x,t)$, and natural decay of angiostatin (with characteristic decay time T_a).

leads to the following system of differential equations:

$$\frac{\partial v}{\partial t} = -\frac{\lambda_1 \delta_e v p}{1+\nu_1 v} + v_r(x,t) \tag{7}$$

$$\frac{\partial c}{\partial t} = \frac{\lambda_1 \delta_e v p}{1+\nu_1 v} - \mu c \tag{8}$$

$$\frac{\partial f}{\partial t} = \frac{4}{T_f} f\left(1-\frac{f}{f_0}\right)\frac{p}{p_0} - \lambda_3 c_a f \tag{9}$$

$$\frac{\partial a}{\partial t} = a_r(x,t) - \frac{a}{T_a}. \tag{10}$$

Note that only the active protease, c_a, takes part in the degradation of fibronectin, and we have

$$c_a = \frac{c}{1+\nu_e a + \nu_3 f}. \tag{11}$$

Diffusion has been neglected here as it takes place on a much longer time scale than the kinetic reactions in the capillary. However, it is necessary to include diffusion terms for the VEGF, fibronectin and angiostatin in the ECM.

Although EC will continue to secrete fibronectin in the ECM, there will also be fibronectin synthesis by cells residing throughout the ECM, primarily fibroblasts (Clark *et al.*, 1982). We therefore use a logistic growth law that is independent of P for fibronectin synthesis in the ECM.

The exogenously supplied angiostatin, in addition to being delivered to the parent capillary, will be delivered to the new capillaries. The trajectories of the new capillaries will correspond to areas where the ECM has been degraded by the migrating EC (Pepper, 2001). We therefore include an angiostatin source term, $a_r(x,t)\left(1-\frac{F}{f_0}\right)$ (Levine *et al.*, 2001a).

†EC exhibit a strong tendency to secrete ECM components, such as fibronectin (Birdwell *et al.*, 1978; Clark *et al.*, 1981). Note, however, that no secretion will take place until proteolysis has reduced the fibronectin concentration below its initial level of f_0. Only once the EC have been activated, and angiogenesis is underway, will fibronectin secretion begin (Clark *et al.*, 1982).

Thus we have the following system of PDEs in the ECM†.

$$\frac{\partial V}{\partial t} = D_V \nabla^2 V - \frac{\lambda_1 \delta_e V P}{1 + \nu_1 V} \tag{12}$$

$$\frac{\partial C}{\partial t} = \frac{\lambda_1 \delta_e V P}{1 + \nu_1 V} - \mu C \tag{13}$$

$$\frac{\partial F}{\partial t} = D_F \nabla^2 F + \frac{4}{T_F} F \left(1 - \frac{F}{f_0}\right) - \lambda_3 C_A F \tag{14}$$

$$\frac{\partial A}{\partial t} = D_A \nabla^2 A + a_r\,(x, t) \left(1 - \frac{F}{f_0}\right) - \frac{A}{T_a} \tag{15}$$

where D_V, D_F, D_A and T_F are constants.

The active protease law also applies in the ECM:

$$C_A = \frac{C}{1 + \nu_e A + \nu_3 F}. \tag{16}$$

2.2 *The cell movement equations*

In the quiescent endothelium, connections between neighbouring EC are tight and there is little or no cell movement (Han & Liu, 1999). However, during angiogenesis, cell–cell connections are loosened and EC are observed to migrate towards the tumour (Ausprunk & Folkman, 1977; Carmeliet, 2000). It is therefore important to account for EC movement.

We assume that the EC lining the capillary wall move on a regular mesh (of mesh size h). Let $p_n\,(t)$ be the EC density at mesh point n at time t. Let $\hat{\tau}_n^{\pm}$ be the transition rate of EC moving from mesh point n to mesh point $n \pm 1$.

Consider the master equation for the EC:

$$\frac{\partial p_n}{\partial t} = \hat{\tau}_{n-1}^{+} p_{n-1} + \hat{\tau}_{n+1}^{-} p_{n+1} - \left(\hat{\tau}_n^{+} + \hat{\tau}_n^{-}\right) p_n. \tag{17}$$

Assume that the decision ‘when to move’ is independent of the decision ‘where to move’ (Othmer & Stevens, 1997). Then the mean waiting time at a mesh point is constant.

So let

$$\hat{\tau}_n^{+} + \hat{\tau}_n^{-} = 2\lambda \tag{18}$$

for λ constant.

†The sink term in (12) represents uptake and binding of VEGF by the actively migrating EC in the ECM, whereas the corresponding term in (7) represents uptake and binding of VEGF by EC in the parent vessel. We emphasize this distinction since the parent capillary is regarded as a mature vessel with a well defined barrier (the basement membrane) which chemical species must cross in order to enter or leave the circulation, whereas in the ECM, the migrating EC have an immature phenotype and there is no basement membrane separating them from diffusing proteins. VEGF may therefore be bound directly by EC in the ECM, via the uptake term in (12), but must first cross the capillary wall (see boundary condition (31) below) before it may be bound by EC in the parent vessel, via (7).

Further assume that the transition probabilities depend only on the control substances at the 'nearest $\frac{1}{2}$ neighbour' mesh points, and let

$$\hat{\tau}_n^{\pm}(w) = 2\lambda \frac{\tau\left(w_{n\pm 1/2}\right)}{\tau\left(w_{n-1/2}\right) + \tau\left(w_{n+1/2}\right)} \equiv 2\lambda N_n^{\pm}(w) \tag{19}$$

where w is the vector of control substances.

The master equation now reads

$$\frac{1}{2\lambda}\frac{\partial p_n}{\partial t} = N_{n-1}^{+} p_{n-1} + N_{n+1}^{-} p_{n+1} - p_n. \tag{20}$$

It can be shown (Othmer & Stevens, 1997) that the continuum limit, $h \to 0$, $\lambda \to \infty$ (such that $\lambda h^2 = D_p$) of (20) is

$$\frac{\partial p}{\partial t} = D_p \frac{\partial}{\partial x}\left(p \frac{\partial}{\partial x}\left(\ln \frac{p}{\tau}\right)\right). \tag{21}$$

Levine *et al.* (2001a) took $\tau = \tau(c_a, f)$ and did not include any dependence on VEGF. However, the exact roles of the various control substances are not fully understood and the appropriate form for τ is unclear. In an attempt to investigate the functions of the control substances, we take $\tau = \tau(c_a, f, v)$ and look at various possibilities for the exact form of τ.

VEGF is a potent chemoattractant for EC (Klagsbrun & D'Amore, 1996) and so EC will migrate towards regions of high VEGF concentration. Similarly, protease will be expressed, in response to VEGF, in areas of angiogenic activity, and so we assume that protease also has a chemotactic effect on the EC.

The effect of ECM components, such as fibronectin, on the directional movement of cells is unclear and there is conflicting experimental evidence. Some authors have reported migration of cells up fibronectin concentration gradients (Bowersox & Sorgente, 1982). However, others have suggested that proteolytic fragments of fibronectin may act as chemoattractants for EC, which will consequently migrate to areas of tissue degradation, where the fibronectin concentration is low (Nicosia *et al.*, 1993). Furthermore, undegraded extracellular tissue represents a significant barrier to cell movement *in vivo* and, during angiogenesis, EC secrete proteolytic enzymes to degrade the ECM, facilitating migration (Pepper *et al.*, 1990; Pepper, 2001). Taking fibronectin concentration as a measure of the penetrability of the tissue, we therefore take the view that EC are attracted to regions of *low* fibronectin. They will thus move towards areas where the ECM has been degraded, and where they can hence move more freely.

Hence $\tau(c_a, f, v)$ should be an increasing function of c_a and v and a decreasing function of f. In order to avoid singularities in $\ln \tau$ and its derivatives, we take

$$\tau(c_a, f, v) = \left(\frac{c_a + \alpha_1}{c_a + \alpha_2}\right)^{\gamma_1} \left(\frac{f + \beta_1}{f + \beta_2}\right)^{\gamma_2} \left(\frac{v + \delta_1}{v + \delta_2}\right)^{\gamma_3}, \tag{22}$$

where $0 < \alpha_1, \delta_1 \ll 1 < \alpha_2, \delta_2$, $0 < \beta_2 \ll 1 < \beta_1$ and $\gamma_1, \gamma_2, \gamma_3 > 0$.

The chemotactic sensitivity associated with this choice is

$$\frac{\tau_x}{\tau} = \gamma_1 \frac{\alpha_2 - \alpha_1}{(c_a + \alpha_1)(c_a + \alpha_2)} \frac{\partial c_a}{\partial x} + \gamma_2 \frac{\beta_2 - \beta_1}{(f + \beta_1)(f + \beta_2)} \frac{\partial f}{\partial x} + \gamma_3 \frac{\delta_2 - \delta_1}{(v + \delta_1)(v + \delta_2)} \frac{\partial v}{\partial x}$$

which reflects the fact that cells become desensitized to chemotactic gradients when the concentration of the control substance is high (Anderson & Chaplain, 1998).

The two-dimensional version of the master equation governing cell movement in the ECM is

$$\frac{1}{4\lambda}\frac{\partial P_{n,m}}{\partial t} = N^{H+}_{n-1,m}P_{n-1,m} + N^{H-}_{n+1,m}P_{n+1,m} + N^{V+}_{n,m-1}P_{n,m-1} + N^{V-}_{n,m+1}P_{n,m+1} - P_{n,m} \tag{23}$$

where

$$N^{H\pm}_{n,m} = \frac{T\left(w_{n\pm 1/2,m}\right)}{T\left(w_{n-1/2,m}\right) + T\left(w_{n+1/2,m}\right) + T\left(w_{n,m-1/2}\right) + T\left(w_{n,m+1/2}\right)}$$

$$N^{V\pm}_{n,m} = \frac{T\left(w_{n,m\pm 1/2}\right)}{T\left(w_{n-1/2,m}\right) + T\left(w_{n+1/2,m}\right) + T\left(w_{n,m-1/2}\right) + T\left(w_{n,m+1/2}\right)}$$

and the superscripts, H and V, denote movement in the horizontal and vertical directions respectively.

The continuum limit of the two-dimensional master equation is

$$\frac{\partial P}{\partial t} = D_P \nabla\cdot\left(P\nabla\left(\ln\frac{P}{T}\right)\right). \tag{24}$$

In addition to migration, EC proliferation is an important component of angiogenesis (Paweletz & Kneirim, 1989). We therefore add a proliferation term, Γ, to the master equation (23):

$$\Gamma = P\left[\left(Q + G\left(C_A\right)\frac{\partial C_A}{\partial t}\right) - \mu_1\right], \tag{25}$$

where $Q, \mu_1 > 0$ are constants. The method used to incorporate this term into simulations based on the master equation (23) is discussed in Section 3.

The first term inside the square brackets represents EC proliferation; the second represents natural death by apoptosis (programmed cell death) (Liu *et al.*, 2000). The QP term represents a constant (low) level of background proliferation, whilst the $G\left(C_A\right)$ term represents a protease-dependent contribution to cell proliferation. Proteolytic enzymes have two opposing effects on EC (Levine *et al.*, 2001a): low concentrations of protease are observed to stimulate proliferation (Carney & Cunningham, 1977); high concentrations result in cell disintegration and death. Thus the proliferation response fraction, $\Theta \equiv \frac{P(t)-P(0)}{P(0)}$, will initially increase with active protease, but will subsequently fall off to zero as the active protease concentration becomes high (Unemori *et al.*, 1992). We therefore choose

$$\Theta = AC_A \exp\left(-\lambda_0 C_A^{m_1}\right)$$

(see Fig. 3) where A, λ_0 and m_1 are positive constants.

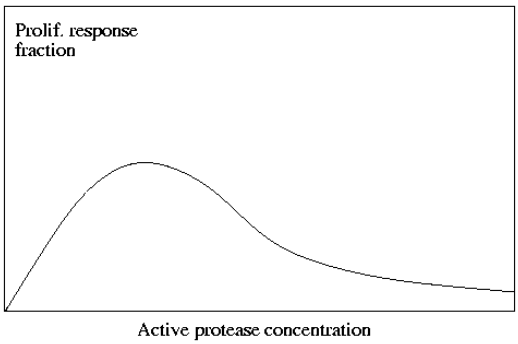

FIG. 3. Proliferation response curve.

Note that one can write $P(t) = P(0)(1+\Theta)$ and so $P'(t) = P(0)\Theta'\frac{\partial C_A}{\partial t}$. Eliminating $P(0)$ yields $P'(t) = P\frac{\Theta'}{1+\Theta}\frac{\partial C_A}{\partial t}$. We therefore choose

$$G(C_A) = \frac{\Theta'(C_A)}{1+\Theta(C_A)} = \frac{A\exp\left(-\lambda_0 C_A^{m_1}\right)\left(1-\lambda_0 m_1 C_A^{m_1}\right)}{1+AC_A\exp\left(-\lambda_0 C_A^{m_1}\right)}. \tag{26}$$

We take $T(C_A, F, V)$ to be of the same form as in the capillary:

$$T(C_A, F, V) = \left(\frac{C_A+\alpha_3}{C_A+\alpha_4}\right)^{\gamma_4}\left(\frac{F+\beta_3}{F+\beta_4}\right)^{\gamma_5}\left(\frac{V+\delta_3}{V+\delta_4}\right)^{\gamma_6}, \tag{27}$$

where $0 < \alpha_3, \delta_3 \ll 1 < \alpha_4, \delta_4, 0 < \beta_4 \ll 1 < \beta_3$ and $\gamma_4, \gamma_5, \gamma_6 > 0$.

We use the master equations (20) and (23), along with rules for branching and looping (see Section 3), to simulate the behaviour of individual EC in the capillary and the ECM respectively. The continuum limit PDEs (21) and (24) are only included to demonstrate the link between the continuum and discrete models that is provided by the reinforced random walk framework, *and are not solved numerically in the simulations*.

2.3 *Initial, boundary and transmission conditions*

For the model to function as required, the ECM and capillary equations must be coupled by appropriate transmission conditions. The rate of supply of VEGF to the capillary, $v_r(x,t)$, is assumed to depend on the difference between the VEGF concentration just outside the capillary wall, $V(x,0,t)$, and in the capillary, $v(x,t)$ (Levine *et al.*, 2001a).

$$v_r(x,t) = B_1(V(x,0,t) - v(x,t)) \tag{28}$$

for $B_1 \geqslant 0$ constant.

Angiostatin is supplied intravenously, at a constant rate, after an initial period, T_{iv}:

$$a_r(x,t) = A_r H(t - T_{iv}). \tag{29}$$

Furthermore, it is assumed that EC cannot move into the ECM until the fibronectin concentration in the capillary falls below a certain threshold level, f_1. The fibronectin concentration in the capillary, $f(x,t)$, is viewed as a measure of the penetrability of the basement membrane: a high concentration corresponding to an intact and impenetrable membrane; a low concentration corresponding to a degraded membrane. The EC must proteolytically degrade the basement membrane before they can escape from the parent vessel into the ECM (Pepper, 1997). We therefore assume that an EC can only move from the capillary to the ECM once the local fibronectin concentration has fallen below the threshold level, f_1. This may be written mathematically:

$$P(x,0,t) = H(f_1 - f(x,t))\, p(x,t). \tag{30}$$

We need boundary conditions for the VEGF, fibronectin and angiostatin. Across the interface between the capillary and the ECM, we assume that there is no flux of fibronectin, and that the flux of VEGF and angiostatin is proportional to the difference between the concentrations in the capillary and in the ECM. Boundary conditions at the capillary side of the ECM are therefore taken as follows[†]:

$$-D_V \frac{\partial V(x,0,t)}{\partial y} + \psi\,(V(x,0,t) - v(x,t)) = 0 \tag{31}$$

$$-D_F \frac{\partial F(x,0,t)}{\partial y} = 0 \tag{32}$$

$$-D_A \frac{\partial A(x,0,t)}{\partial y} + \psi'\,(A(x,0,t) - a(x,t)) = 0 \tag{33}$$

for ψ,ψ' constant.

At the tumour side of the ECM, we need to introduce a source of VEGF, $V_l(x,t)$. We assume that there is no flux of EC, fibronectin or angiostatin and thus take the following boundary conditions:

$$-D_P \frac{\partial}{\partial y}\left(\ln \frac{P}{T}\right)(x,l,t) = 0 \tag{34}$$

$$-D_V \frac{\partial V(x,l,t)}{\partial y} = -V_l(x,t) \tag{35}$$

$$-D_F \frac{\partial F(x,l,t)}{\partial y} = 0 \tag{36}$$

$$-D_A \frac{\partial A(x,l,t)}{\partial y} = 0. \tag{37}$$

The source function is taken to be a unimodal function, normalized so that the total flux over the boundary $y = l$ is v_0 (Levine *et al.*, 2001a):

$$V_l(x,t) = \frac{v_0 \sigma}{L}\left(1 - \cos\frac{2\pi x}{L}\right)^{m_0}, \tag{38}$$

[†]One could include a dependence of the transport terms (31), (33) on the 'thickness' of the basement membrane, $f(x,t)$, thereby slightly increasing the VEGF supply to the parent capillary as the basement membrane is degraded. The effect of this would be to reduce the time until the EC first escape from the parent capillary.

where $\sigma = \left(\int_0^1 (1-\cos 2\pi x)^{m_0}\,\mathrm{d}x\right)^{-1}$ and $v_0 > 0$ is a constant.

We also impose no-flux boundary conditions at $x = 0, L$:

$$D_P P \frac{\partial}{\partial x}\left(\ln\frac{P}{T}\right)(0,y,t) = D_P P \frac{\partial}{\partial x}\left(\ln\frac{P}{T}\right)(L,y,t) = 0 \tag{39}$$

$$D_p p \frac{\partial}{\partial x}\left(\ln\frac{p}{\tau}\right)(0,t) = D_p p \frac{\partial}{\partial x}\left(\ln\frac{p}{\tau}\right)(L,t) = 0 \tag{40}$$

$$D_V \frac{\partial V(0,y,t)}{\partial x} = D_V \frac{\partial V(L,y,t)}{\partial x} = 0 \tag{41}$$

$$D_F \frac{\partial F(0,y,t)}{\partial x} = D_F \frac{\partial F(L,y,t)}{\partial x} = 0 \tag{42}$$

$$D_A \frac{\partial A(0,y,t)}{\partial x} = D_A \frac{\partial A(L,y,t)}{\partial x} = 0. \tag{43}$$

Initially, there is a uniform distribution of EC in the capillary, and a uniform distribution of fibronectin in both the capillary and the ECM. All other quantities are zero. The initial conditions are therefore

$$\begin{array}{ll} p(x,0) = p_0 & P(x,y,0) = 0 \\ v(x,0) = 0 & V(x,y,0) = 0 \\ f(x,0) = f_0 & F(x,y,0) = f_0 \\ c(x,0) = 0 & C(x,y,0) = 0 \\ a(x,0) = 0 & A(x,y,0) = 0. \end{array} \tag{44}$$

Note that, for the simulations, we have taken the fibronectin concentration in the capillary (representing the thickness of the basement membrane) to be equal to that in the ECM. It is possible that the basement membrane represents a more significant obstacle for the EC than does ordinary extracellular tissue. This would suggest that f_0 should be greater in the capillary than in the ECM and the effects of this will be discussed in Section 4.

2.4 *Non-dimensionalization*

Set $p' = \frac{p}{p_0}$, $P' = \frac{P}{p_0}$, $p'_m = \frac{p_m}{p_0}$, $v' = \nu_1 v$, $V' = \nu_1 V$, $f' = \frac{f}{f_0}$, $F' = \frac{F}{f_0}$, $c' = \nu_1 c$, $C' = \nu_1 C$, $a' = \nu_e a$, $A' = \nu_e A$, $x' = \frac{x}{L}$, $y' = \frac{y}{L}$, $t' = \frac{D_p}{L^2}t$, $\lambda' = \frac{L^2}{h^2}$. The constants resulting from this scaling are rewritten in the following as K_i (see Table 1).

The system (7)–(11), (20), (22) becomes (dropping the dashes)

$$\frac{\partial p_n}{\partial t} = 2\lambda\left(N^+_{n-1}p_{n-1} + N^-_{n+1}p_{n+1} - p_n\right) \tag{45}$$

$$\frac{\partial v}{\partial t} = -K_1\frac{vp}{1+v} + K_2\left(V(x,0,t) - v(x,t)\right) \tag{46}$$

$$\frac{\partial c}{\partial t} = K_1\frac{vp}{1+v} - K_3 c \tag{47}$$

$$\frac{\partial f}{\partial t} = K_4 f(1-f)\,p - K_5 c_a f \tag{48}$$

$$\frac{\partial a}{\partial t} = K_7 H(t - K_8) - K_9 \tag{49}$$

$$\tau\left(c_a,\, f,\, v\right) = \left(\frac{c_a + K_{10}}{c_a + K_{11}}\right)^{\gamma_1} \left(\frac{f + K_{12}}{f + K_{13}}\right)^{\gamma_2} \left(\frac{v + K_{14}}{v + K_{15}}\right)^{\gamma_3} \tag{50}$$

$$c_a = \frac{c}{1 + a + K_6 f}. \tag{51}$$

Similarly, the ECM equations (12)–(16), (23), (25)–(27) become

$$\begin{aligned}\frac{\partial P_{n,m}}{\partial t} = {} & 4\lambda \left(N^{H+}_{n-1,m} P_{n-1,m} + N^{H-}_{n+1,m} P_{n+1,m} + N^{V+}_{n,m-1} P_{n,m-1}\right. \\ & \left. + N^{V-}_{n,m+1} P_{n,m+1} - P_{n,m}\right) \\ & + P_{n,m}\left[\left(K_{18} + \bar{G}\left(C_A\right)\frac{\partial C_A}{\partial t}\right) - K_{20}\right]\end{aligned} \tag{52}$$

$$\frac{\partial V}{\partial t} = K_{21}\nabla^2 V - K_1 \frac{VP}{1+V} \tag{53}$$

$$\frac{\partial C}{\partial t} = K_1 \frac{VP}{1+V} - K_3 C \tag{54}$$

$$\frac{\partial F}{\partial t} = K_{22}\nabla^2 F + K_{23} F\left(1 - F\right) - K_5 C_A F \tag{55}$$

$$\frac{\partial A}{\partial t} = K_{24}\nabla^2 A + K_7 H\left(t - K_8\right)\left(1 - F\right) - K_9 A \tag{56}$$

$$\bar{G}\left(C_A\right) = K_{25} \frac{e^{-K_{26} C_A^{m_1}}\left(1 - K_{26} m_1 C_A^{m_1}\right)}{1 + K_{25} C_A e^{-K_{26} C_A^{m_1}}} \tag{57}$$

$$T\left(C_A, F, V\right) = \left(\frac{C_A + K_{27}}{C_A + K_{28}}\right)^{\gamma_4} \left(\frac{F + K_{29}}{F + K_{30}}\right)^{\gamma_5} \left(\frac{V + K_{31}}{V + K_{32}}\right)^{\gamma_6} \tag{58}$$

$$C_a = \frac{C}{1 + A + K_6 F}. \tag{59}$$

The boundary conditions (30)–(43) become

$$P\left(x, 0, t\right) = H\left(\frac{f_1}{f_0} - f\left(x, t\right)\right) p\left(x, t\right) \tag{60}$$

$$-K_{33}\frac{\partial V\left(x, 0, t\right)}{\partial y} + V\left(x, 0, t\right) = v\left(x, t\right) \tag{61}$$

$$\frac{\partial F\left(x, 0, t\right)}{\partial y} = 0 \tag{62}$$

$$-K_{34}\frac{\partial A\left(x, 0, t\right)}{\partial y} + A\left(x, 0, t\right) = a\left(x, t\right) \tag{63}$$

$$P\frac{\partial}{\partial y}\left(\ln\frac{P}{T}\right)(x, l/L, t) = 0 \tag{64}$$

$$\frac{\partial V(x, l/L, t)}{\partial y} = K_{35}(1 - \cos(2\pi x))^{m_0} \tag{65}$$

$$\frac{\partial F(x, l/L, t)}{\partial y} = 0 \tag{66}$$

$$\frac{\partial A(x, l/L, t)}{\partial y} = 0 \tag{67}$$

$$P\frac{\partial}{\partial x}\left(\ln\frac{P}{T}\right)(0, y, t) = P\frac{\partial}{\partial x}\left(\ln\frac{P}{T}\right)(1, y, t) = 0 \tag{68}$$

$$p\frac{\partial}{\partial x}\left(\ln\frac{p}{\tau}\right)(0, t) = p\frac{\partial}{\partial x}\left(\ln\frac{p}{\tau}\right)(1, t) = 0 \tag{69}$$

$$\frac{\partial V(0, y, t)}{\partial x} = \frac{\partial V(1, y, t)}{\partial x} = 0 \tag{70}$$

$$\frac{\partial F(0, y, t)}{\partial x} = \frac{\partial F(1, y, t)}{\partial x} = 0 \tag{71}$$

$$\frac{\partial A(0, y, t)}{\partial x} = \frac{\partial A(1, y, t)}{\partial x} = 0. \tag{72}$$

Finally, the initial conditions (44) take the form

$$\begin{array}{ll} p(x, 0) = 1 & P(x, y, 0) = 0 \\ v(x, 0) = 0 & V(x, y, 0) = 0 \\ f(x, 0) = 1 & F(x, y, 0) = 1 \\ c(x, 0) = 0 & C(x, y, 0) = 0 \\ a(x, 0) = 0 & A(x, y, 0) = 0. \end{array} \tag{73}$$

3. Method of simulation

Cell movement is governed by the master equations (17) and (23). For each cell at each time step, the probabilities of staying still, and moving in each direction are calculated.

In the capillary, the probabilities are given, as in Othmer & Stevens (1997), by (19)

$$\begin{aligned} P(\text{stay still}) &= 1 - 2\lambda k \\ P(\text{move left}) &= 2\lambda k\frac{\tau_{n-1/2}}{\tau_{n-1/2} + \tau_{n+1/2}} \\ P(\text{move right}) &= 2\lambda k\frac{\tau_{n+1/2}}{\tau_{n-1/2} + \tau_{n+1/2}}. \end{aligned}$$

TABLE 1 *Constants resulting from the non-dimensionalization of the model.*

i	K_i	i	K_i	i	K_i
1	$\frac{L^2\lambda_1\delta_e p_0}{D_p}$	2	$\frac{L^2 B_1}{D_p}$	3	$\frac{L^2\mu}{D_p}$
4	$\frac{4L^2}{D_p T_f}$	5	$\frac{L^2\lambda_3}{D_p\nu_1}$	6	$f_0\nu_3$
7	$\frac{\nu_e A_r L^2}{D_p}$	8	$\frac{D_p T_{iv}}{L^2}$	9	$\frac{L^2}{D_p T_a}$
10	$\alpha_1\nu_1$	11	$\alpha_2\nu_1$	12	$\frac{\beta_1}{f_0}$
13	$\frac{\beta_2}{f_0}$	14	$\delta_1\nu_1$	15	$\delta_2\nu_1$
		17	$\frac{D_P}{D_p}$	18	$\frac{L^2 Q}{D_p}$
		20	$\frac{L^2\mu_1}{D_p}$	21	$\frac{D_V}{D_p}$
22	$\frac{D_F}{D_p}$	23	$\frac{4L^2}{D_p T_F}$	24	$\frac{D_A}{D_p}$
25	$\frac{A}{\nu_1}$	26	$\frac{\lambda_0}{\nu_1^{m_1}}$	27	$\alpha_3\nu_1$
28	$\alpha_4\nu_1$	29	$\frac{\beta_3}{f_0}$	30	$\frac{\beta_4}{f_0}$
31	$\delta_3\nu_1$	32	$\delta_4\nu_1$	33	$\frac{D_V}{L\psi}$
34	$\frac{D_A}{L\psi'}$	35	$\frac{v_0\sigma\nu_1}{D_V}$		

In the ECM, the probabilities are

$$
\begin{aligned}
P\text{ (stay still)} &= 1 - 4\lambda k \\
P\text{ (move left)} &= 4\lambda k \frac{T_{n-1/2,m}}{T_{n-1/2,m} + T_{n+1/2,m} + T_{n,m-1/2} + T_{n,m+1/2}} \\
P\text{ (move right)} &= 4\lambda k \frac{T_{n+1/2,m}}{T_{n-1/2,m} + T_{n+1/2,m} + T_{n,m-1/2} + T_{n,m+1/2}} \\
P\text{ (move up)} &= 4\lambda k \frac{T_{n,m-1/2}}{T_{n-1/2,m} + T_{n+1/2,m} + T_{n,m-1/2} + T_{n,m+1/2}} \\
P\text{ (move down)} &= 4\lambda k \frac{T_{n,m+1/2}}{T_{n-1/2,m} + T_{n+1/2,m} + T_{n,m-1/2} + T_{n,m+1/2}}.
\end{aligned}
$$

Using the method of Sleeman & Wallis (2002), the interval [0, 1) is then divided into three (or in the ECM, five) intervals of length corresponding to the above probabilities. A random number is generated in [0, 1) and depending into which probability interval the random number falls, the cell either stays still or moves accordingly.

Proliferation and death are included by assuming that at any given time step, each cell has a probability $\alpha^+(C_A, P) \geqslant 0$ of dividing and $\alpha^-(C_A, P) \geqslant 0$ of dying. Then the expected increase, in one time step, of the cell density at mesh point (n, m) is $\left(\alpha^+ - \alpha^-\right) P$. Hence by (52), we must have

$$
\left(\alpha^+ - \alpha^-\right) P = kP\left[\left(K_{18} + \bar{G}\left(C_A\right)\frac{\partial C_A}{\partial t}\right) - K_{20}\right]. \tag{74}
$$

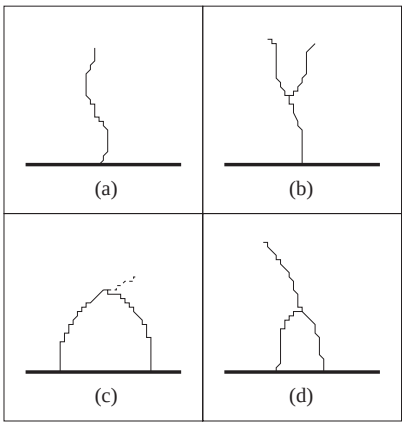

FIG. 4. Schematic diagram of developing capillaries: (a) a migrating capillary tip; (b) a capillary branch; (c) tip-to-tip anastomosis; (d) tip-to-branch anastomosis.

Of the three terms on the right-hand side of (74), the background proliferation term, K_{18}, is always non-negative, the apoptosis term, $-K_{20}$, is always negative and the protease-dependent term, $\bar{G}(C_A)\frac{\partial C_A}{\partial t}$ can be positive or negative. We wish to satisfy (74) in such a way that α^+ is composed of the positive (or proliferative) terms and α^- of the negative (or death) terms.

In the case $\bar{G}(C_A)\frac{\partial C_A}{\partial t} \geqslant 0$, this term contributes to cell proliferation and should therefore be included in α^+. We therefore satisfy (74) as follows:

$$\alpha^+(C_A, P) = \left(kK_{18} + \bar{G}(C_A)(C_A(t) - C_A(t-k))\right)$$
$$\alpha^-(C_A, P) = kK_{20}.$$

If $\bar{G}(C_A)\frac{\partial C_A}{\partial t} < 0$, this term contributes to cell death and so needs to be included in α^-. In this case we express (74) as

$$\alpha^+(C_A, P) = kK_{18}$$
$$\alpha^-(C_A, P) = \left(kK_{20} - \bar{G}(C_A)(C_A(t) - C_A(t-k))\right).$$

In the capillary, cell aggregation is allowed (i.e. more than one cell is permitted to occupy a single mesh point) as this may be one mechanism by which the cells move together to degrade the capillary wall. In the ECM, however, each cell is viewed as a 'leader' cell, tracing the trajectory of a newly forming capillary tip (Fig. 4(a)). Other EC, not included in the model, are assumed to follow the path of this leader to form the capillary lumen. When a cell divides, a new cell is created and the capillary branches (Fig. 4(b)); when a cell dies, the capillary tip can move no further. When a cell collides with another cell, we have a tip-to-tip anastomosis (Paweletz & Kneirim, 1989): a closed loop is formed and only one of the capillary tips continues (Fig. 4(c)). When a cell collides with the *trail* of another, we have a tip-to-branch anastomosis and the colliding capillary tip ceases to move (Fig. 4(d)).

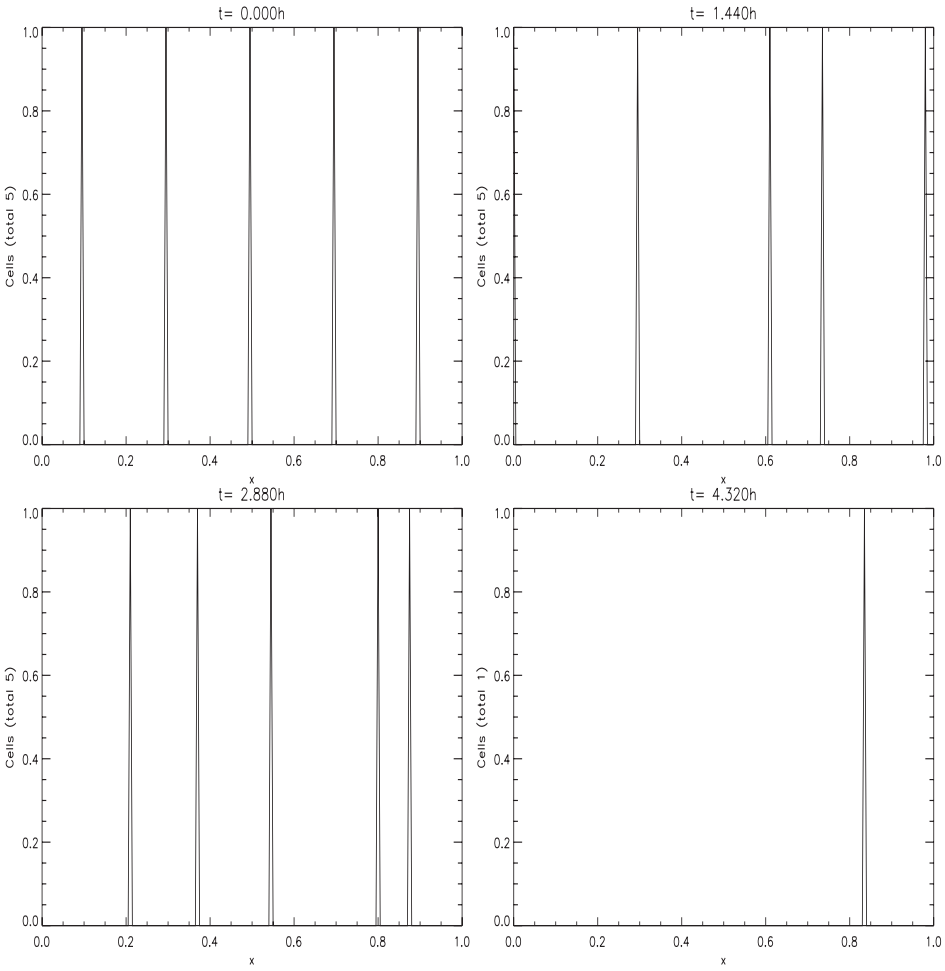

FIG. 5. Positions of the EC in the capillary.

4. Results and discussion

Simulations of the system (46)–(50), (53)–(73) were run, together with the rules for individual cell movement and capillary branching and looping described in Section 3. For a discussion of the parameter values involved, see Appendix B; unless stated otherwise, these are the values used in the simulations. The first few simulations do *not* include angiostatin (i.e. $A_r = 0$ in (29)).

Taking the average length of an EC to be 0·01 mm (Levine *et al.*, 2001a), the 0·05 mm section of capillary being modelled here will consist of approximately five cells. Figure 5 shows the positions of (the centres of) the five cells in the capillary at $t = 0$ h, $t = 1{\cdot}44$ h, $t = 2{\cdot}88$ h and $t = 4{\cdot}32$ h. Figures 6–8 show how the substrate profiles evolve in the

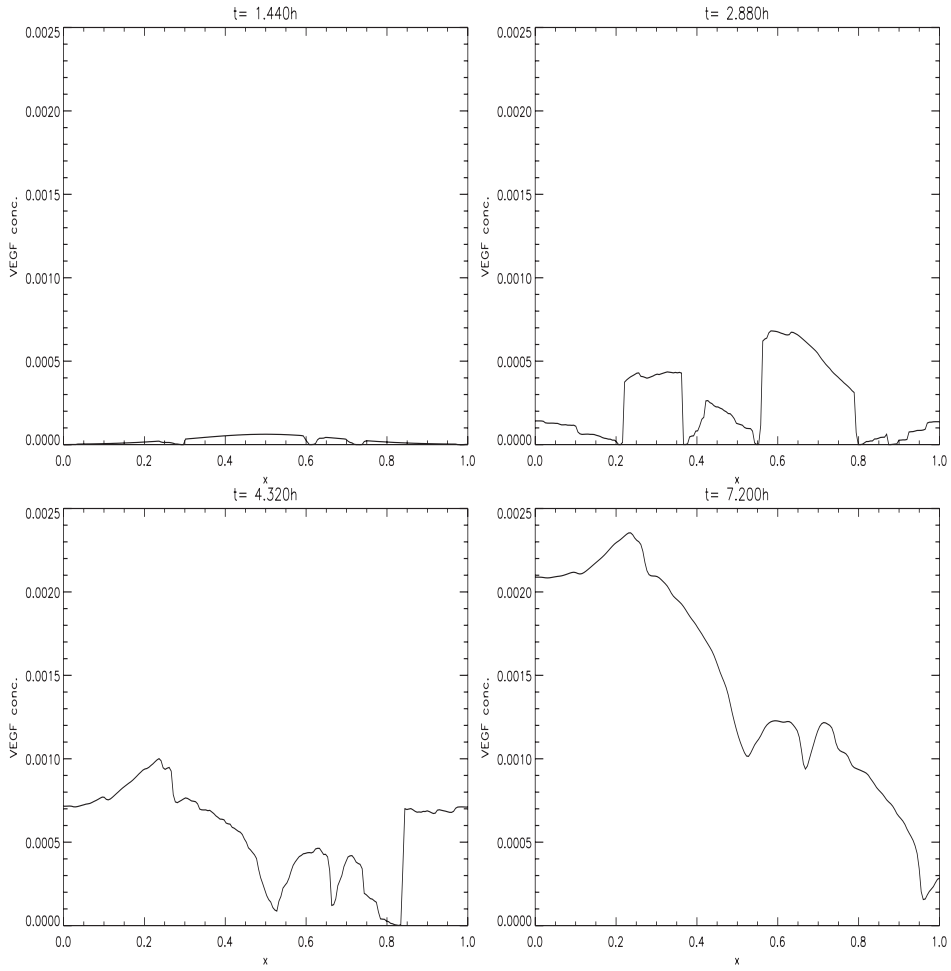

FIG. 6. Evolution of the VEGF profile in the capillary.

capillary. Figure 9 shows the trails formed by EC in the ECM and Figs 10–12 show how the substrates evolve in the ECM.

In Fig. 5, the cells begin at equally spaced points along the capillary and subsequently begin to move. In Figs 6 and 7, one can see the uptake of VEGF by the EC and the resulting production of protease (at $t = 0$, there is no VEGF or protease in the capillary). The positions of the cells thus correspond to areas where VEGF has been taken up and protease has been synthesized. Figure 8 shows how the protease then degrades the fibronectin in the capillary wall (at $t = 0$ the fibronectin is equal to 1 everywhere). As soon as the fibronectin density falls below the threshold level of 0·6, the cells can move out of the capillary into the ECM. This first happens at $t = 4{\cdot}32$ h, by which time two 'holes', (one large one between $x = 0{\cdot}3$ and $x = 0{\cdot}65$ and one smaller one at approximately $x = 0{\cdot}75$) have been cut in the fibronectin. Four of the five cells have escaped through these holes into the ECM. By

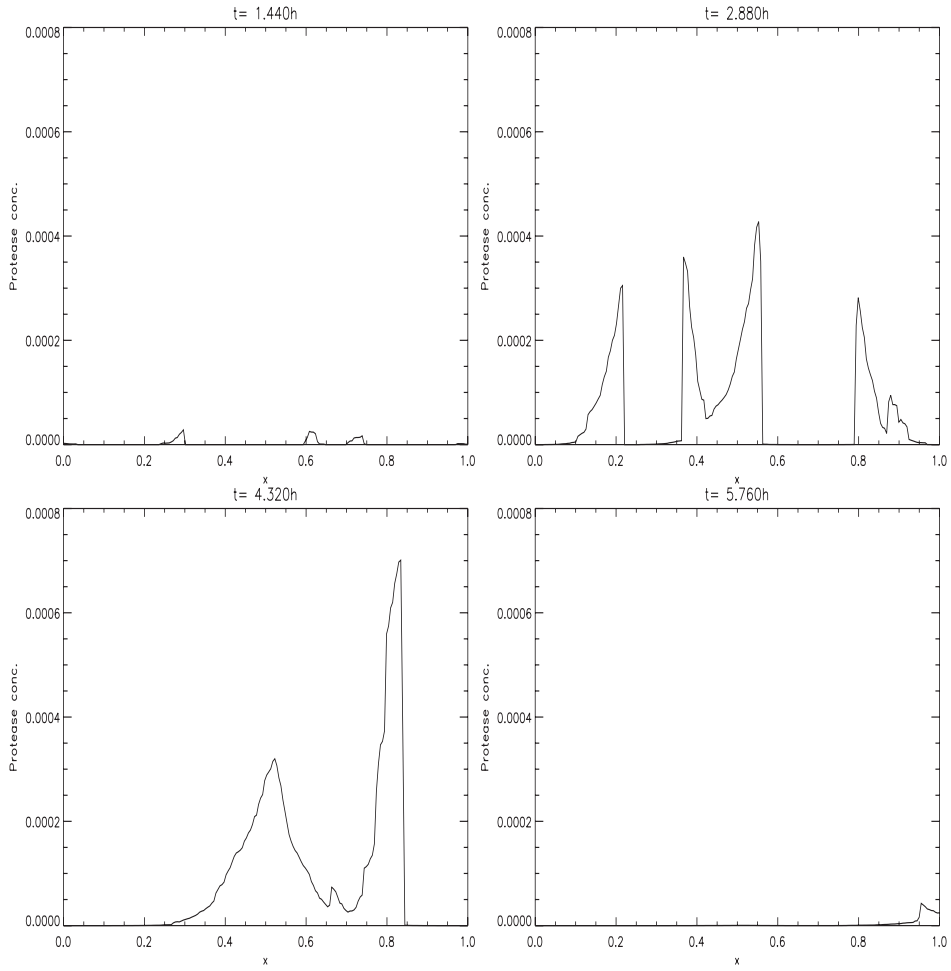

FIG. 7. Evolution of the protease profile in the capillary.

the next snapshot ($t = 7{\cdot}20$ h), a third hole has been made and the one remaining cell is able to escape from the capillary.

In Fig. 9, one sees how the cells migrate across the ECM towards the tumour, forming a capillary network as they go. Recall that only the leading EC are simulated and a capillary is assumed to grow in the path of each lead cell. Note that there are only four capillaries sprouting from the parent vessel, despite the fact that five cells began the simulation. The reason for this is that two of the cells aggregated in the capillary and, when the fibronectin concentration fell below the threshold level, were occupying the same point. They then moved into the ECM together and immediately fused, leaving just one leading cell, forming a single capillary sprout. Vessel branching is already apparent in Fig. 9 at $t = 4{\cdot}32h$, contributing to the number of migrating capillary tips. The formation of closed capillary loops (anastomosis), which is necessary for blood flow to begin, is in evidence

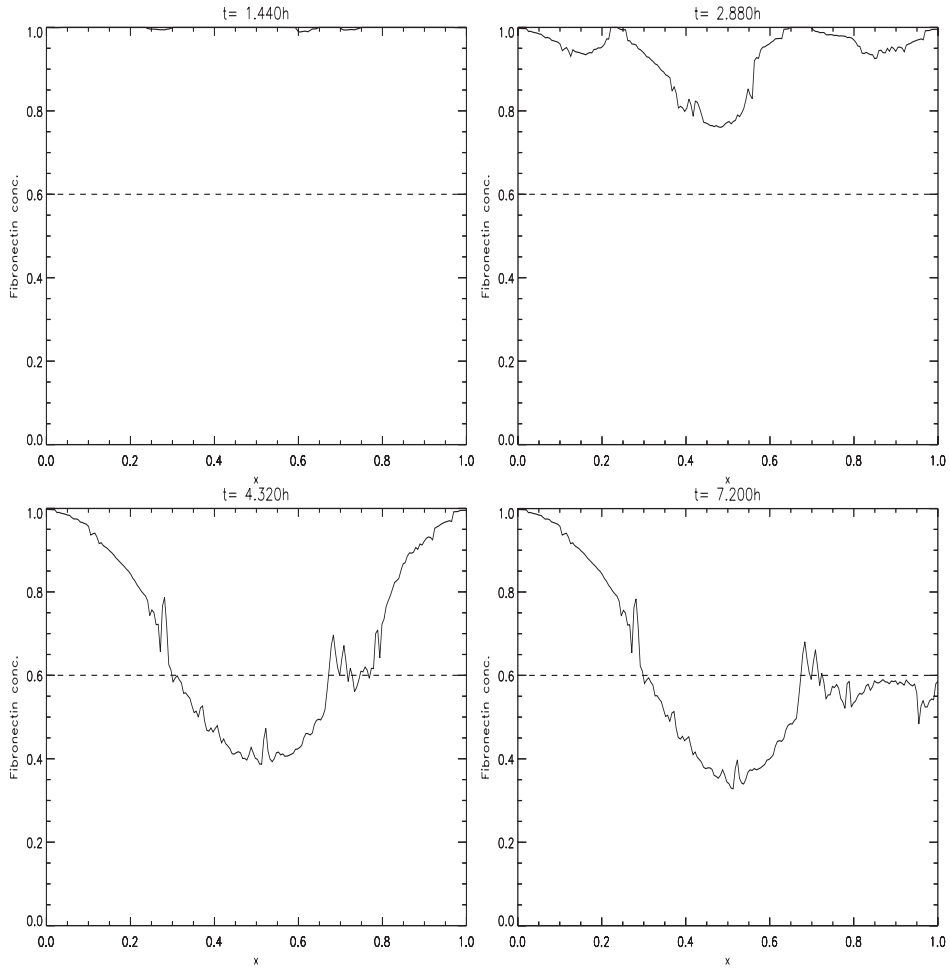

FIG. 8. Evolution of the fibronectin profile in the capillary (the dashed line indicates the threshold level of fibronectin).

by $t = 5{\cdot}76$ h. Also at $t = 5{\cdot}76$ h, the first migrating cells have reached the tumour (an event which shall be referred to as 'the onset of vascularization') and angiogenesis has succeeded. Angiogenic activity continues to take place between $t = 5{\cdot}76$ h and $t = 7{\cdot}20$ h, resulting in a more extensive vascular network, with a greater number of capillaries making contact with the tumour. There is also some migration of EC back towards the parent vessel, most notably on the left-hand side of the domain. This phenomenon has been observed experimentally (Muthukkaruppan & Auerbach, 1979), and in other mathematical models (Holmes & Sleeman, 2000), and may be one mechanism responsible for the formation of closed loops.

Figure 10 shows how the VEGF is taken up by the EC as they migrate towards the tumour. Up until $t = 2{\cdot}88$ h, all five cells are still in the capillary, and the VEGF profile

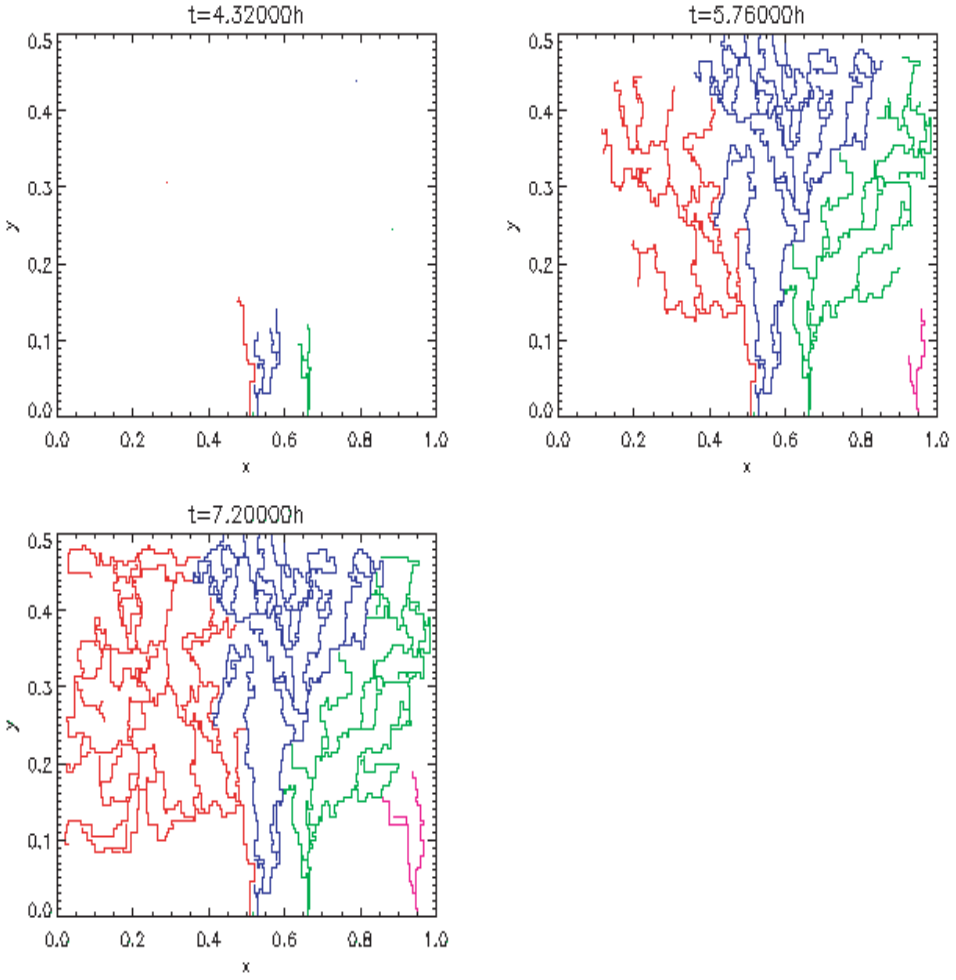

FIG. 9. Trails formed by the EC as they migrate across the ECM (the capillary is at $y = 0$ and the tumour is centred at $(x, y) = (0{\cdot}5, 0{\cdot}5)$).

is smooth and diffusion-dominated. At $t = 4{\cdot}32$ h, there is a small number of cells in the ECM, and small irregularities are visible in the VEGF profile at the position of those cells, indicating VEGF uptake. At $t = 5{\cdot}76$ h, there are many more cells in the ECM and VEGF uptake is much more pronounced, with a significant region in which all VEGF has been taken up. By $t = 7{\cdot}20$ h, a diffusion-dominated profile has started to re-establish itself. This is because the bulk of the angiogenic activity has already taken place by this time: many cells have reached the tumour, and many others have formed anastomoses, and thus do not take any further part in the simulation.

Figure 11 tells a similar story with regard to the protease evolution. Again, the presence of a few cells in the ECM at $t = 4{\cdot}32$ h is detectable by a small peak of protease. As time

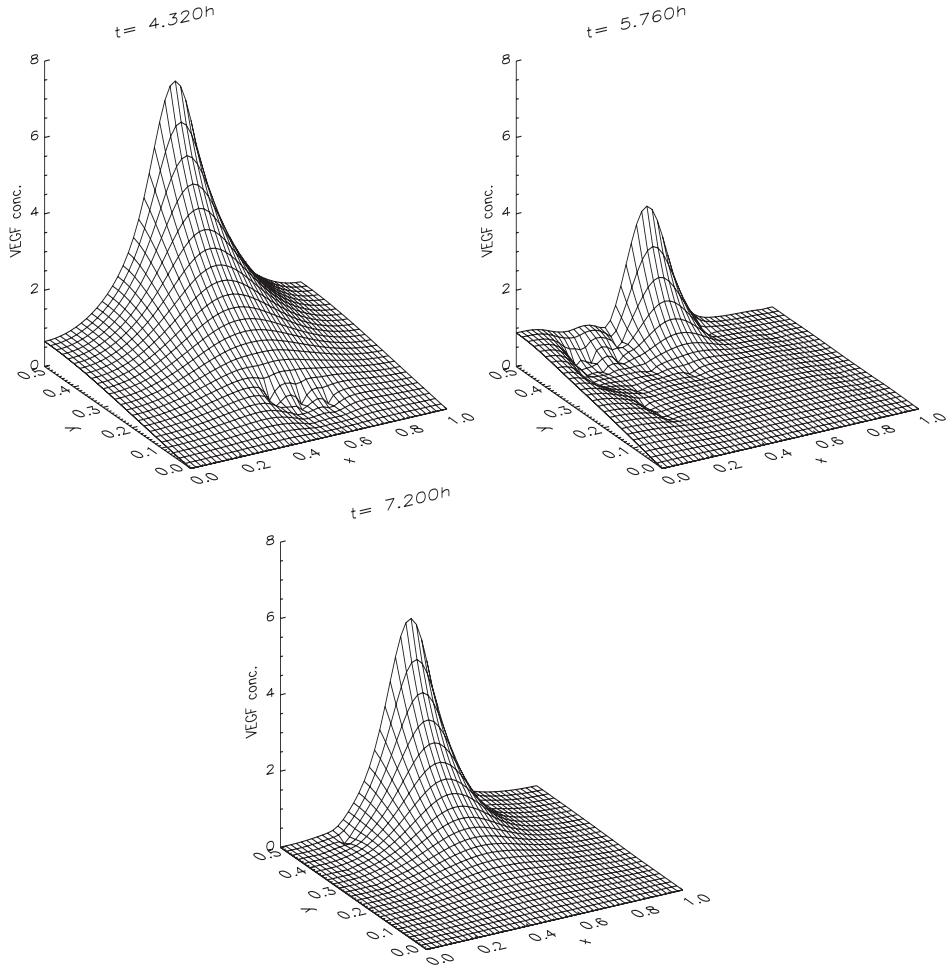

FIG. 10. Evolution of the VEGF profile in the ECM.

progresses, the number of cells increases and protease production levels rise. However, by $t = 7{\cdot}20$ h, protease levels have again fallen because of the decrease in the number of active cells in the ECM.

Finally, Fig. 12 shows the path cut by the cells through the fibronectin. Once again, the cells in the ECM at $t = 4{\cdot}32$ h have started to degrade fibronectin. As time passes and more capillaries start growing, degradation becomes widespread and by $t = 7{\cdot}20$ h, the fibronectin profile has been decimated.

Note that, in the simulations, the background fibronectin level, f_0, is the same in the capillary as in the ECM. As remarked in Section 2.3, one could choose f_0 to be greater in the capillary than the ECM, represent a thicker basement membrane. Unsurprisingly, simulations run with this choice (not shown) indicate that the greater f_0 in the capillary, the longer it takes for the EC to degrade the fibronectin to the threshold level. Hence the

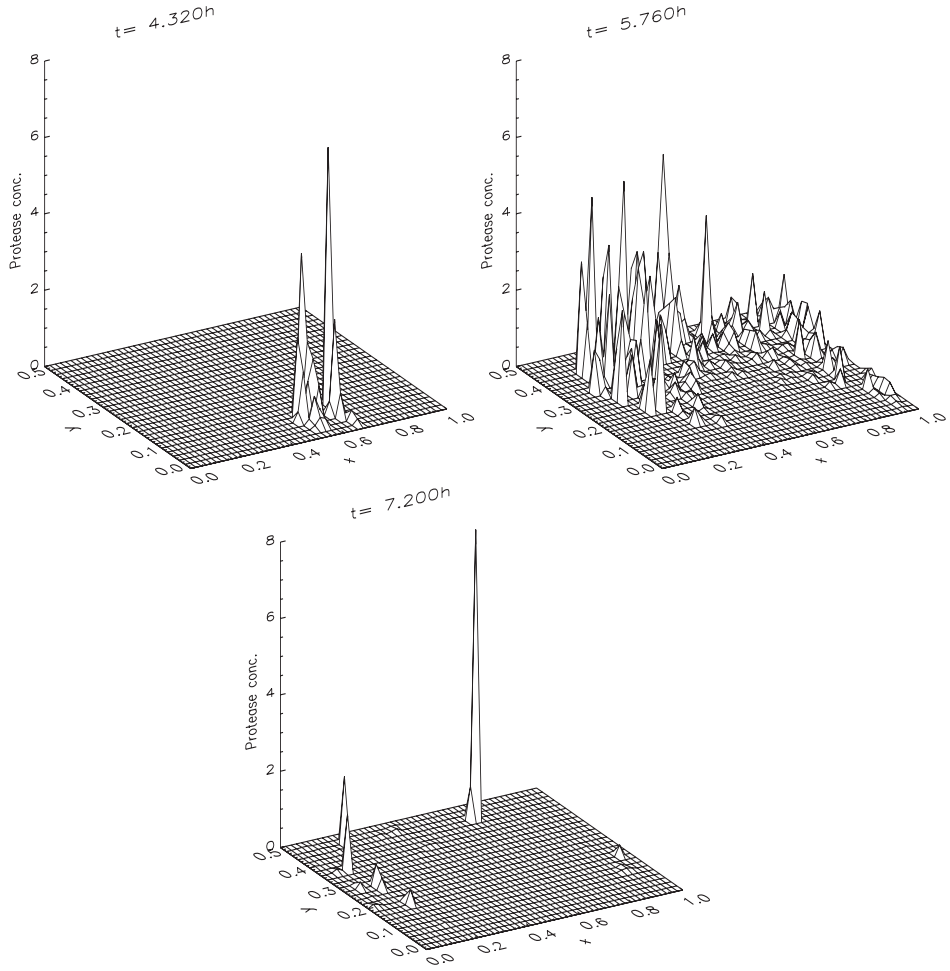

FIG. 11. Evolution of the protease profile in the ECM.

thicker the basement membrane, the more difficult it is for EC of the parent vessel to extravasate and begin to form new vessels.

Figure 13 shows a simulation in which EC proliferation is *not* included ($\Gamma = 0$ in (25)). The fact that there are only four migrating capillary tips is again due to cell aggregation in the capillary prior to extravasation. In the ECM, there is, as expected, little network formation with no capillary branching and only one anastomosis. The migrating tips do not reach the tumour and vascularization does not take place within 7·20 h. It is well known (Sholley *et al.*, 1984; Paweletz & Kneirim, 1989) that, although a primitive vascular network can form under the action of EC migration alone, proliferation is required for the formation of a fully functional network and the successful completion of angiogenesis. Thus the model is in agreement with experimental observations on this point: initial capillary sprouting occurs as normal but subsequent vascular growth is limited.

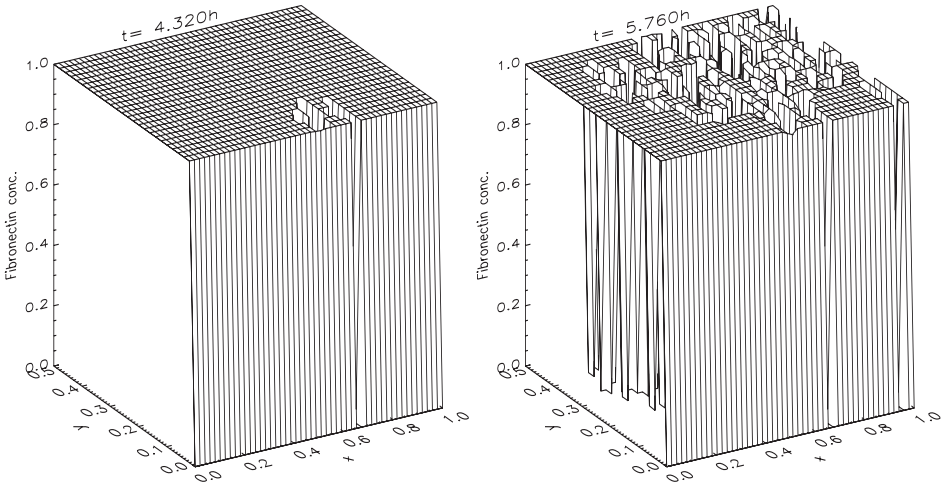

FIG. 12. Evolution of the fibronectin profile in the ECM.

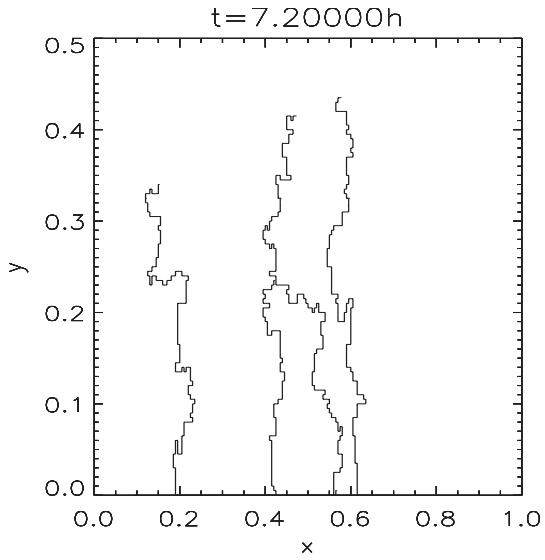

FIG. 13. Trails formed in the absence of EC proliferation.

VEGF is the main regulatory factor by which tumours elicit an angiogenic response from the host (Yancopoulos *et al.*, 2000). To investigate further the role of VEGF, we carried out simulations with various levels of VEGF expression by the tumour. Figure 14 shows a simulation with a reduced VEGF source term ($v_0 = 0{\cdot}01\mu$M mm^2 h^{-1} in (38)). This results in a greatly reduced angiogenic response, with delayed extravasation (EC did not escape the parent capillary until $t = 6{\cdot}55$ h) and very little migration, branching or looping. Further reduction of the VEGF source term leads to a failure of the EC to escape

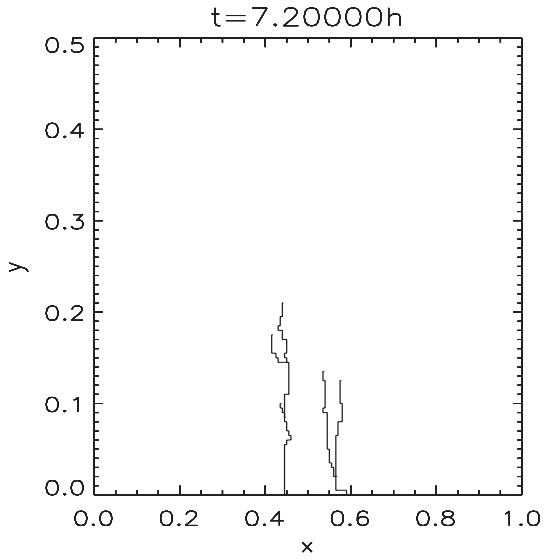

FIG. 14. Trails formed with a reduced VEGF source term ($v_0 = 0{\cdot}01\mu$M mm^2 h^{-1}).

the parent capillary (results not shown). These results are consistent with the fact that VEGF is the main driving force behind angiogenesis (Vernon & Sage, 1999; Yancopoulos *et al.*, 2000).

Figure 15 shows a simulation with $v_0 = 0{\cdot}2\mu$M mm^2 h^{-1} (i.e. VEGF *increased* by a factor of 5 from its standard level). As one would expect, this increases the angiogenic response. Extravasation and vascularization take place earlier and vessel branching and looping is more pronounced, resulting in a denser capillary network.

In Fig. 16, the source of VEGF is increased further ($v_0 = 2{\cdot}0\mu$M mm^2 h^{-1}). Although the capillaries initially grow much more rapidly than in Fig. 9, with prolific branching and looping, there is an area around the tumour in which there is no capillary formation whatsoever: vascularization has not taken place. There are two possible reasons for this. The first is that, as mentioned in Section 2.2, the cells become desensitized to chemotactic gradients when the concentration of the chemoattractant is high. It is possible that the high levels of VEGF in the immediate vicinity of the tumour (see Fig. 17) are causing a marked reduction in the chemotactic migration of the cells towards the tumour. The second reason is that the high levels of VEGF are stimulating the EC to produce large quantities of protease (see Fig. 18). By (25), the proliferation response of the cells initially increases with protease but subsequently peaks and will then fall off as the protease concentration increases further. The avascular region in Fig. 16 could correspond to the area where protease production is too great, leading to cell death. The most likely scenario is that it is a combination of these two factors that is causing this effect.

A phenomenon similar to this, termed the brush-border effect (Muthukkaruppan *et al.*, 1982; Byrne & Chaplain, 1995) has been observed in *in vivo* studies of tumour angiogenesis. Branching is seen to increase as the new capillaries approach the tumour, but the vessels do not initially enter the immediate vicinity of the tumour. There thus remains a

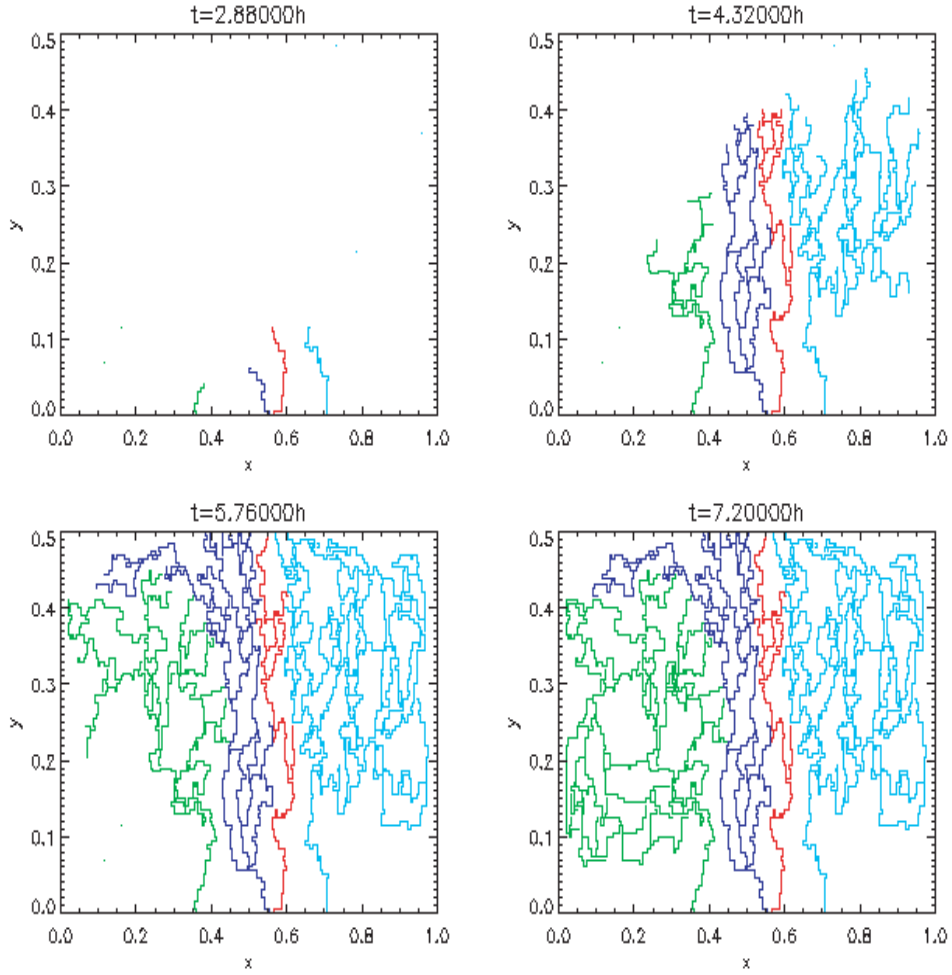

FIG. 15. Trails formed with an increased VEGF source term ($v_0 = 0{\cdot}2\mu$M mm^2 h^{-1}).

narrow band of avascular tissue surrounding the tumour. This appears to be consistent with the results of this model. Moreover, we hypothesize that the reason for the brush-border effect is that the EC encounter an excess of VEGF in the neighbourhood of the tumour. This leads to saturation of the VEGF receptors on the cell surface and the EC lose the ability to detect the VEGF gradient. It may also stimulate excess protease production, leading to cell death.

Figure 19 shows a simulation with $v_0 = 40\mu$M mm^2 h^{-1} (i.e. VEGF increased by a factor of 1000 from its standard level). Although the cells are very quick to escape from the capillary (0·92 h), there is subsequently very limited migration and the EC do not reach the tumour. By $t = 3{\cdot}91$ h, all the leading EC have died and vascular growth stops completely. The cells presumably enter the type of environment that existed near to the

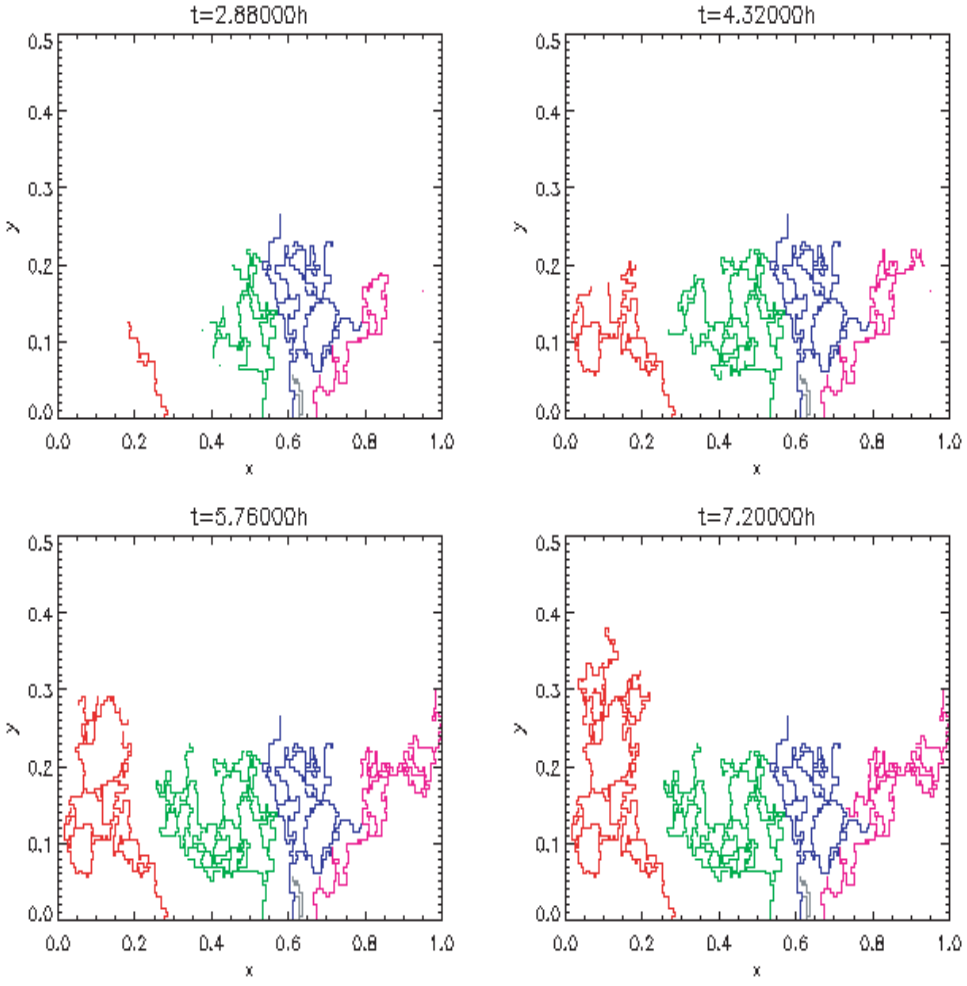

FIG. 16. Trails formed when $v_0 = 2{\cdot}0\mu$M mm^2 h^{-1}.

tumour in Fig. 16 (i.e. excess VEGF resulting desensitization to the chemotactic gradient and/or excess protease resulting in cell death) immediately on escaping from the parent vessel, thus stunting any capillary growth. The fact that cell death occurs suggests that excess protease is certainly one cause of this lack of angiogenic activity.

It has been established that the spatial and temporal expression of VEGF must be precisely regulated if angiogenesis is to succeed in forming a fully functional capillary network (Han & Liu, 1999). Deletion of the gene encoding VEGF leads to an almost complete absence of vascular development, resulting in early embryonic death (Yancopoulos *et al.*, 2000). Over-expression of VEGF also has adverse effects on the formation of a vascular network, causing hyperpermeability and hyperfusion (Klagsbrun & D'Amore, 1996). This critical dependence on VEGF levels appears to be reflected in the

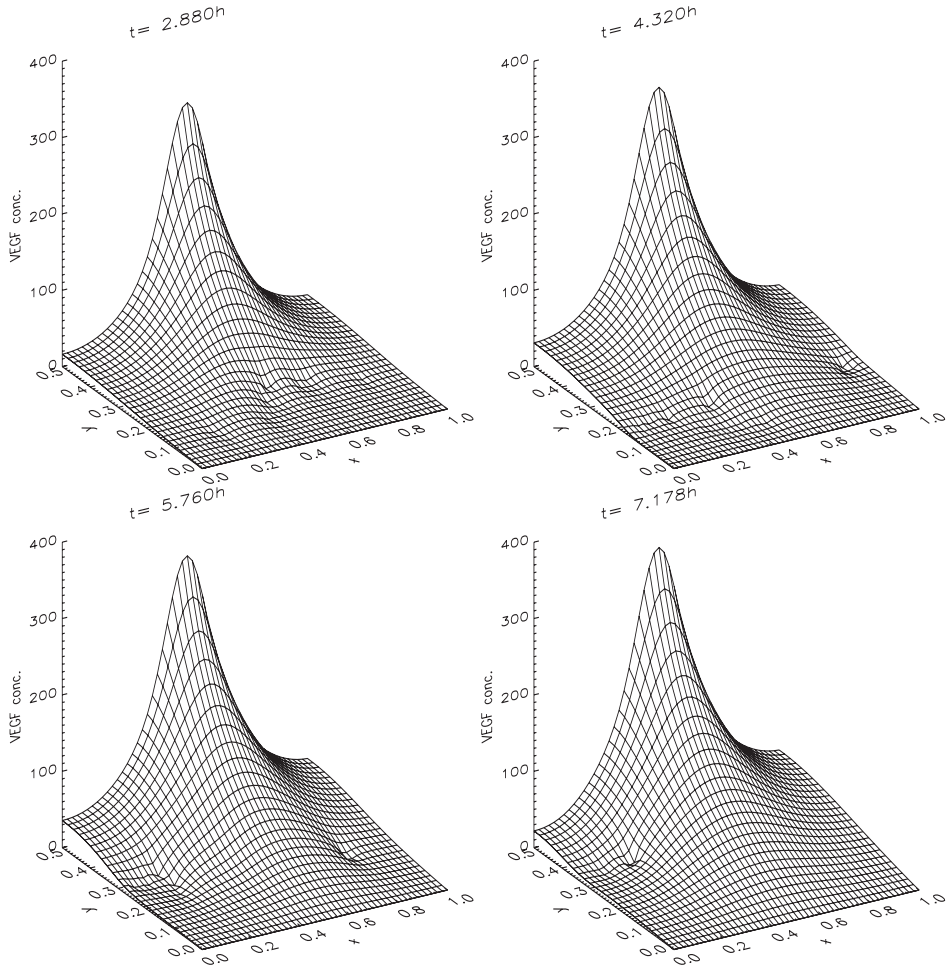

FIG. 17. Evolution of the VEGF profile when $v_0 = 2{\cdot}0\mu\text{M mm}^2\ \text{h}^{-1}$.

results of this model insofar as a relatively small increase in VEGF expression can disrupt angiogenesis in the vicinity of the tumour, whereas a decrease in VEGF expression leads to inadequate EC migration and proliferation.

We now turn our attention to the potential anti-angiogenic effects of angiostatin. Recall that the effect of angiostatin in the model is to deactivate the EC-derived protease, which in turn will affect not only proteolysis of the ECM (14) but also EC migration (23) and proliferation (25). Figure 20 shows a simulation with angiostatin included. The source of angiostatin becomes active at $t = T_{iv} = 4{\cdot}5$ h (29) and so in the first two snapshots, the capillaries are growing normally, under the same conditions as in Fig. 9. However, from that point on, the angiostatin takes effect and angiogenesis proceeds at a slower rate than in Fig. 9 and vascularization does not take place. Concomitantly, the uptake of VEGF (Fig. 21) and the degradation of fibronectin (Fig. 22) do not progress across the ECM as

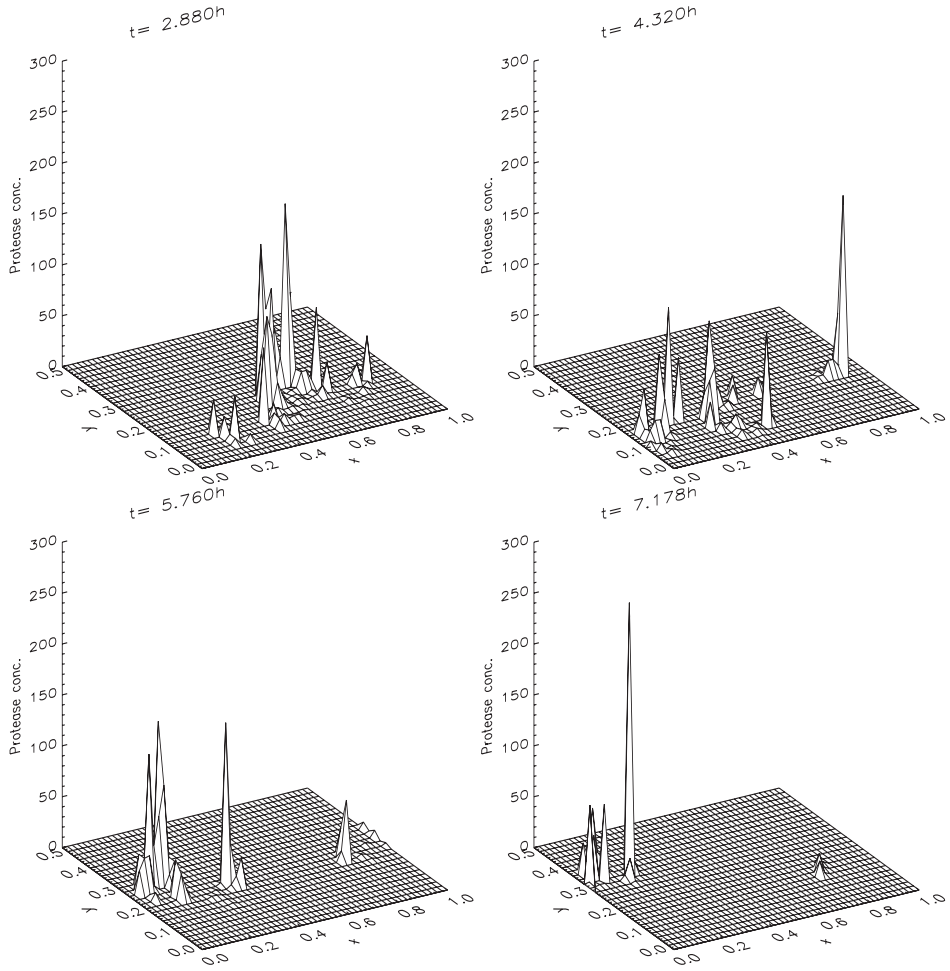

FIG. 18. Evolution of the protease profile when $v_0 = 2{\cdot}0\mu\text{M mm}^2\ \text{h}^{-1}$.

quickly following the introduction of angiostatin. Angiostatin is supplied to the capillary uniformly (49) and to the ECM in areas where the fibronectin is low (56). The angiostatin profile (Fig. 23) shows that the majority of the angiostatin in the ECM arrives by diffusion from the parent capillary. The function of the angiostatin is to deactivate the protease and this can be seen by comparing Fig. 24 (total protease) with Fig. 25 (active protease). Up to $t = 4{\cdot}5$ h, the active protease concentration is the same as the total protease concentration. However, after the introduction of angiostatin, although the total protease concentration grows, active protease remains low and constitutes only a tiny proportion of total protease: by $t = 7{\cdot}2$ h, almost all of the proteolytic enzyme has been deactivated by the action of the angiostatin. It is this reduction of active protease that results in a reduction of the migrating cell population, via the term $\bar{G}\,(C_A)\,\frac{\partial C_A}{\partial t}$ in (25), and thereby prevents the completion of angiogenesis.

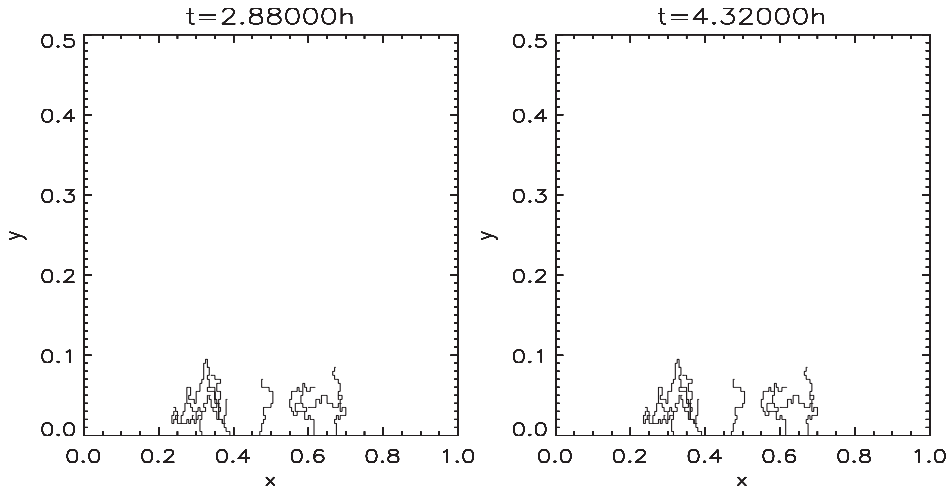

FIG. 19. Trails formed when $v_0 = 40{\cdot}0\mu\text{M mm}^2\ \text{h}^{-1}$.

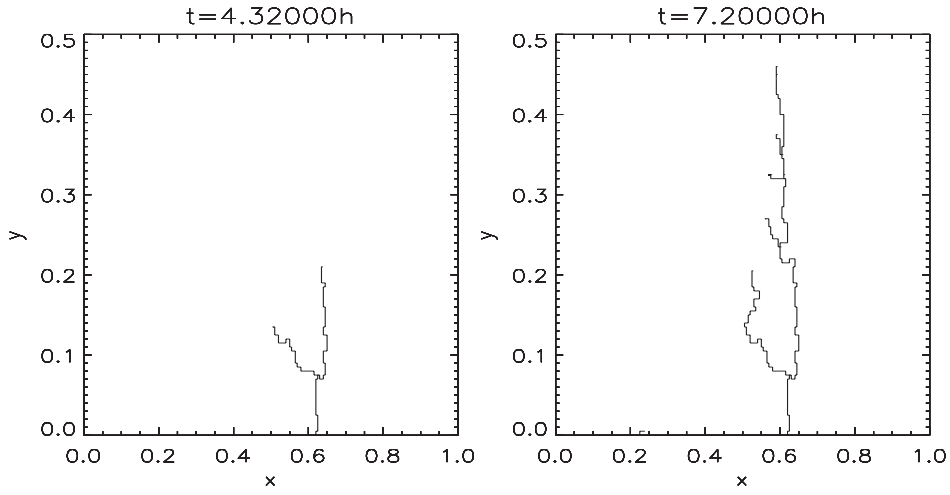

FIG. 20. Trails formed when angiostatin is introduced at $t = 4{\cdot}5$ h.

Figure 26 shows a simulation in which angiostatin is introduced at the earlier time of $T_{iv} = 4$ h and this has successfully reduced angiogenic outgrowth still further with very little capillary formation and no branching or looping. Supplying angiostatin immediately from $T_{iv} = 0$ h prevents extravasation of the EC (results not shown), thus stopping angiogenesis before it starts. It therefore appears that, as one would expect, the earlier angiostatin is introduced, the more effective it will be in preventing angiogenic activity. In particular, if angiostatin can be supplied to the bloodstream before EC have escaped the parent capillary, it will stand a good chance of preventing extravasation because of the dependence of this crucial event on proteolytic activity.

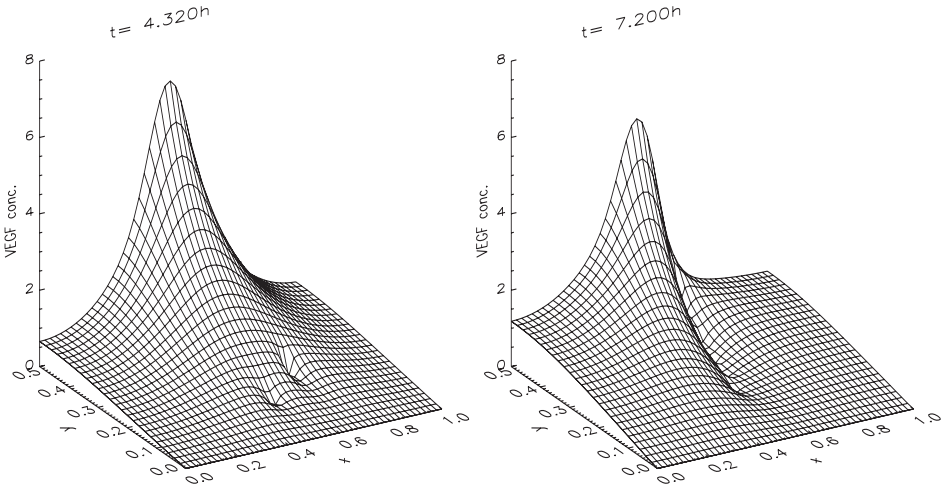

FIG. 21. Evolution of the VEGF profile when angiostatin is introduced at $t = 4{\cdot}5$ h.

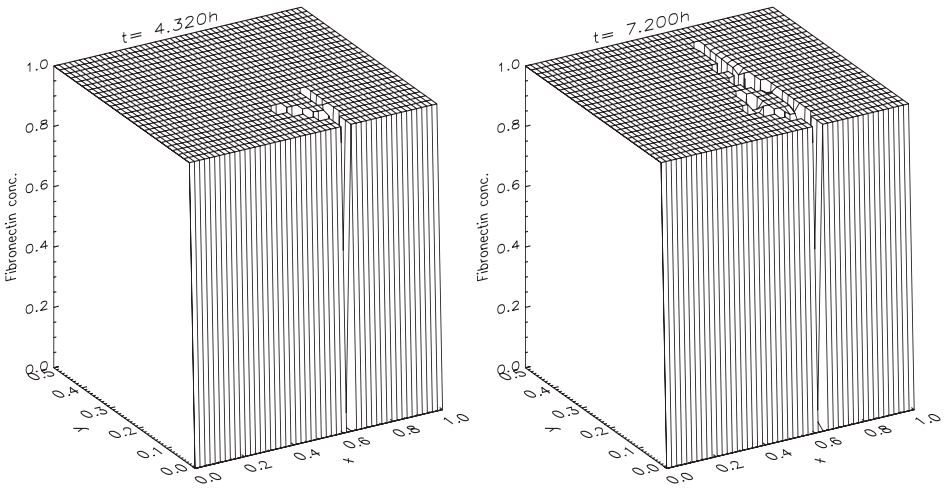

FIG. 22. Evolution of the fibronectin profile when angiostatin is introduced at $t = 4{\cdot}5$ h.

Administration of angiostatin is not the only anti-angiogenic therapy currently undergoing trials (Cao, 2001). Another possible approach would be to prevent VEGF from activating the EC, either by directly inhibiting production of VEGF by the tumour, or via a chemical that blocks the binding of VEGF to the EC receptors (Burke & DeNardo, 2001). To investigate the potential of this approach, we carried out a simulation in which the source of VEGF (38) was curtailed after 4·50 h, so no more VEGF enters the system after this time. Figure 27 shows the resulting capillary formation; Fig. 28 shows the corresponding VEGF profiles. Although the capillaries haven't quite reached the tumour after 7·20 h, they are very close to it and an advanced vascular network has formed

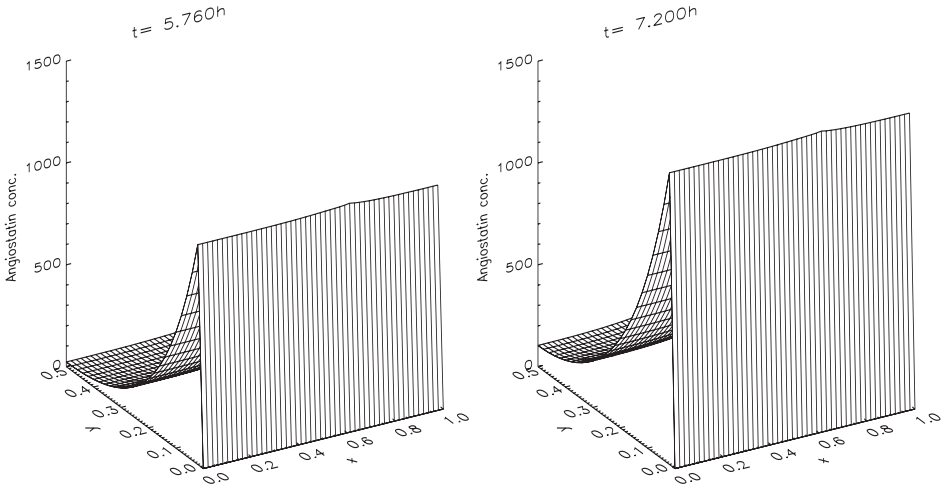

FIG. 23. Evolution of the angiostatin profile.

with many closed loops allowing blood flow. Comparing this with the angiostatin therapy (Fig. 20) would therefore suggest that curtailing the supply of VEGF is not as effective an anti-angiogenic strategy as supplying angiostatin. This may be because, following the removal of the VEGF source, there is a delay while residual VEGF decays (one can see in Fig. 28 that there is still some VEGF remaining at $t = 5{\cdot}76$ h and it is not until $t = 7{\cdot}20$h that VEGF is completely removed from the system). Angiostatin, in contrast, inhibits the proteolytic enzyme as soon as it enters the system, thus having an instant impact on the angiogenic process.

This situation is analogous to the action of the angiopoietins, ligands for the EC receptor tyrosine kinase, Tie-2. Angiopoietin-1 is a stabilizing factor, which helps to keep the capillaries in the quiescent state (Davis *et al.*, 1996). Angiopoietin-2 is an antagonist for Ang-1, binding to the same receptor on EC, but without activating it, thus blocking the effects of Ang-1. Ang-2 is therefore a destabilising factor, which makes the EC more responsive to an angiogenic stimulus (Maisonpierre *et al.*, 1997). The existence of such an agonist–antagonist relationship allows the Tie-2 signalling pathway to be regulated with a high degree of spatial and temporal precision. Simply switching off expression of Ang-1 would be followed by a delay while residual ligand cleared, whereas the ability to express an antagonist, Ang-2, allows instant blocking of the Tie-2 receptor (Jones, 1997).

A comparison of the results presented here with those of a continuum analogue of this model (Levine *et al.*, 2001a) reveals a good qualitative agreement. It will be noticed, however, that the discrete modelling approach has the ability to capture features that are missed by the continuum model. In particular, a better insight can be gained into the microscopic properties of the capillary network which forms in response to the tumour. The branching and looping of the vessels, processes which are not well understood biologically, can be observed directly and the effect of various factors on these processes can be studied. Furthermore, the results of this model show several important similarities with experimental observations. The early events of angiogenesis, namely EC extravasation and

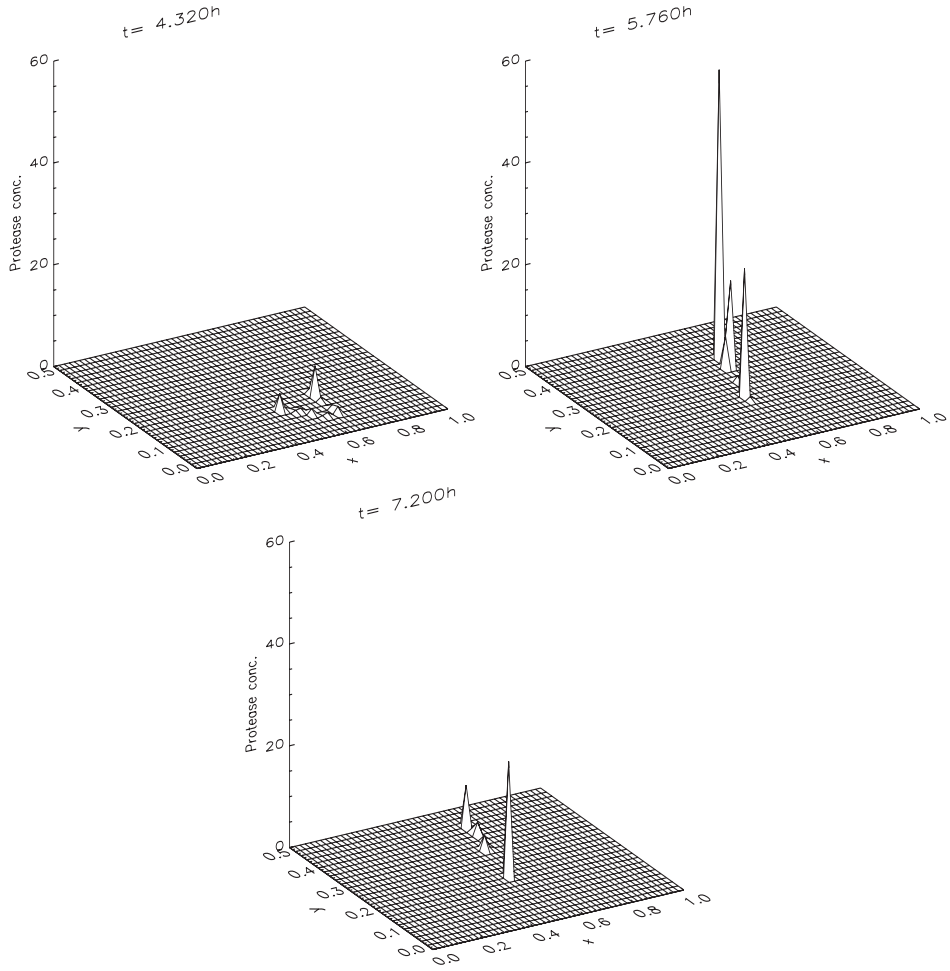

FIG. 24. Evolution of the protease profile when angiostatin is introduced at $t = 4{\cdot}5$ h.

migration, are known to be unaffected by irradiating the EC (thus preventing proliferation), but sustained angiogenic growth does not take place (Sholley *et al.*, 1984). Our results are consistent with this. The formation of a brush-border, another phenomenon that is poorly understood, also appears to occur in our model at a certain level of VEGF production. Angiostatin, an inhibitor of angiogenesis (O'Reilly *et al.*, 1994), which represents a promising anti-angiogenic therapy (Burke & DeNardo, 2001), is capable of preventing vascularization under the assumptions of the model. Our results suggest that, if it can be administered early enough, it would be most effective at preventing the onset of angiogenesis by blocking proteolysis of the basement membrane, which is required for EC extravasation.

This model could be extended in a number of ways. The angiopoietins (see above) have, in recent years, emerged as important regulators of angiogenesis (Jones, 1997), but have yet

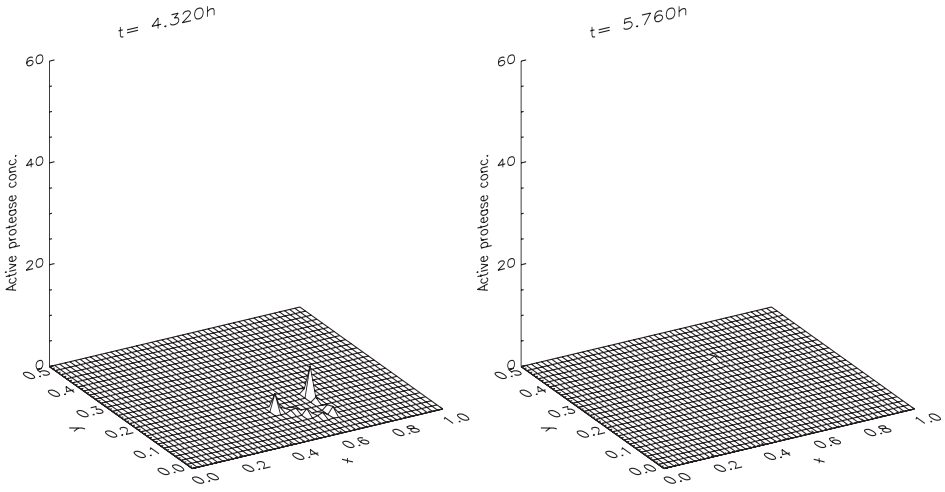

FIG. 25. Evolution of the active protease profile when angiostatin is introduced at $t = 4{\cdot}5$ h.

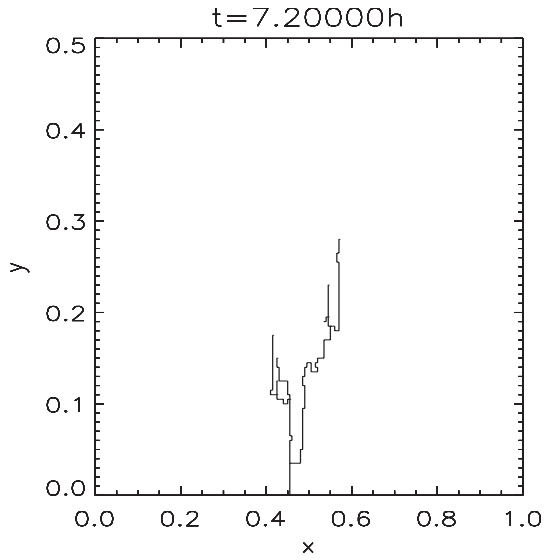

FIG. 26. Trails formed when angiostatin is introduced at $t = 4$ h.

to be incorporated into a mathematical model. Work is currently in progress formulating a continuum model of tumour angiogenesis that includes the actions of the angiopoietins. It is also envisaged that a discrete version of this model could be constructed, in a similar way to the model presented here.

Angiogenesis is a highly complex process, involving a large number of growth factors, growth inhibitors, cell types and ECM components. The biological issues are not fully understood and there is conflicting experimental evidence regarding the roles of some

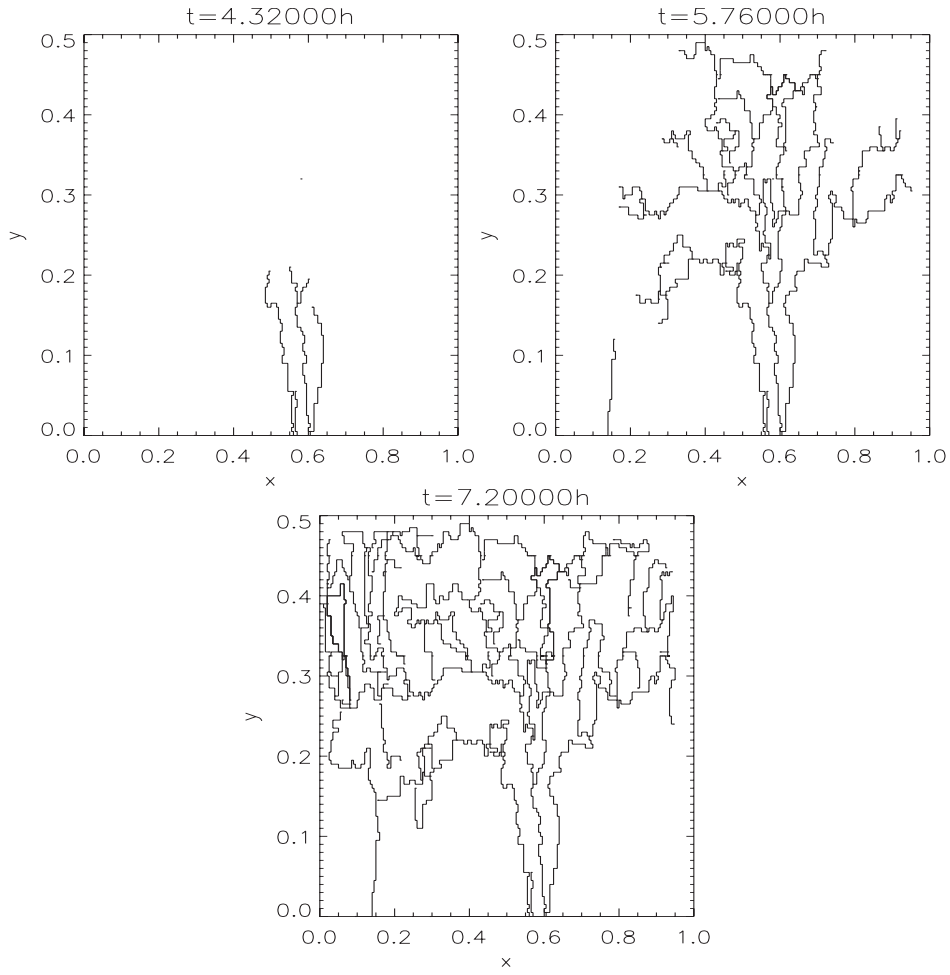

FIG. 27. Trails formed when the source of VEGF is curtailed at $t = 4{\cdot}5$ h.

of the aforementioned players. Here, we have treated the case where angiostatin acts via inhibition of protease, producing knock-on effects on EC migration and proliferation. This was the hypothesis made by Stack *et al.* (1999), but other mechanisms of action are possible, such as induction of EC apoptosis or a direct inhibition of EC migration.

Angiostatin is generated *in vivo* by proteolytic cleavage of plasminogen (Gately *et al.*, 1996). Certain tumour types may express the proteases that are required for this process (Gately *et al.*, 1997). Here we examined the potential anti-angiogenic effects of exogenous angiostatin administration, but tumour-mediated angiostatin generation could be easily incorporated into the model. Indeed, results (not shown) indicate that such a mechanism is capable of inhibiting angiogenesis in the neighbourhood of the tumour. It is questionable whether endogenous angiostatin would be produced in sufficient quantities to have a significant anti-angiogenic effect on the primary tumour. However, the effects of

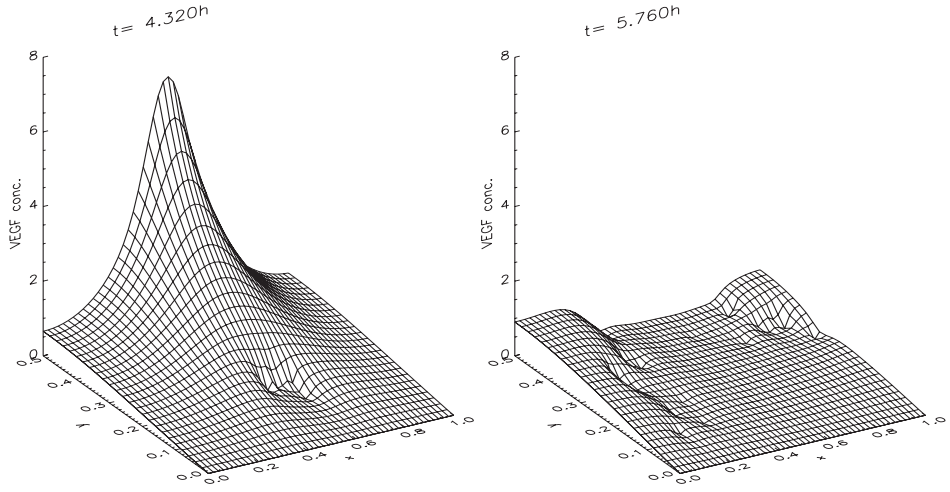

FIG. 28. Evolution of the VEGF profile when the source of VEGF is curtailed at $t = 4{\cdot}5$ h.

long-range inhibition by endogenous angiostatin versus short-range activation by VEGF (see Section 1 and O'Reilly *et al.* (1994)) represent an interesting area for future modelling work.

Another target for future work is to add to the model populations of macrophages and pericytes, which are known to play important roles in tumour angiogenesis, contributing to the production of growth factors and acting as support cells for the capillaries. A continuum model including macrophages and pericytes has been studied by Levine *et al.* (2000) and these additional cell populations could be included in the discrete model via an appropriate master equation.

Acknowledgements

The authors thank Professor H. A. Levine for insightful discussions concerning travel times of EC in the ECM when comparing the predictions of this work with those in Levine *et al.* (2001b). Supported by EPSRC studentship no 00801007.

REFERENCES

ANDERSON, A. R. A. & CHAPLAIN, M. A. J. (1998) Continuous and discrete mathematical models of tumour-induced angiogenesis. *Bull. Math. Biol.*, **60**, 857–900.

ANDERSON, A. R. A., CHAPLAIN, M. A. J., NEWMAN, E. L., STEELE, R. J. C. & THOMPSON, A. M. (2000) Mathematical modelling of tumour invasion and metastasis. *J. Theor. Med.*, **2**, 129–154.

ANDERSON, A. R. A., SLEEMAN, B. D., YOUNG, I. M. & GRIFFITHS, B. S. (1997) Nematode movement along a chemical gradient in a structurally heterogeneous environment: 2. theory. *Fund. Appl. Nematol.*, **20**, 165–172.

AUSPRUNK, D. H. & FOLKMAN, J. (1977) Migration and proliferation of endothelial cells in preformed and newly formed blood vessels during tumour angiogenesis. *Microvasc. Res.*, **14**, 53–65.

BALDING, D. & MCELWAIN, D. L. S. (1985) Mathematical modelling of tumour-induced capillary growth. *J. Theor. Biol.*, **114**, 53–73.

BIRDWELL, C. R., GOSPODAROWICZ, D. & NICOLSON, G. L. (1978) Identification, localisation and role of fibronectin in cultured bovine endothelial cells. *Proc. Natl Acad. Sci. USA*, **75**, 3273–3277.

BOWERSOX, J. C. & SORGENTE, N. (1982) Chemotaxis of aortic endothelial cells in response to fibronectin. *Canc. Res.*, **42**, 2547–2551.

BURKE, P. A. & DENARDO, S. J. (2001) Antiangiogenic agents and their promising potential in combined therapy. *Crit. Rev. Oncol. Hematol.*, **39**, 155–171.

BYRNE, H. M. & CHAPLAIN, M. A. J. (1995) Mathematical models for tumour angiogenesis: numerical simulations and nonlinear wave solutions. *Bull. Math. Biol.*, **57**, 461–486.

CAO, Y. (2001) Endogenous angiogenesis inhibitors and their therapeutic implications. *Int. J. Biochem. Cell Biol.*, **33**, 357–369.

CARMELIET, P. (2000) Mechanisms of angiogenesis and arteriogenesis. *Nature Med.*, **6**, 389–395.

CARMELIET, P. & JAIN, R. K. (2000) Angiogenesis in cancer and other diseases. *Nature*, **407**, 249–257.

CARNEY, D. H. & CUNNINGHAM, D. D. (1977) Initiation of chick cell division by trypsin action at the cell surface. *Nature*, **268**, 602–606.

CARTER, S. B. (1965) Principles of cell motility: the direction of cell movement and cancer invasion. *Nature*, **208**, 1183–1187.

CAVALLARO, U. & CHRISTOFORI, G. (2000) Molecular mechanisms of tumour angiogenesis and tumour progression. *J. Neuro-Oncol.*, **50**, 63–70.

CHAPLAIN, M. A. J., GILES, S. M., SLEEMAN, B. D. & JARVIS, R. J. (1995) A mathematical model for tumour angiogenesis. *J. Math. Biol.*, **33**, 744–770.

CHAPLAIN, M. A. J. & STUART, A. M. (1993) A model mechanism for the chemotactic response of endothelial cells to tumour angiogenesis factor. *IMA J. Math. Appl. Med. Biol.*, **10**, 149–168.

CLAESSON-WELSH, L., WELSH, M., ITO, N., ANAND-APTE, B., SOKER, S., ZETTER, B., O'REILLY, M. & FOLKMAN, J. (1998) Angiostatin induces endothelial cell apoptosis and activation of focal adhesion kinase independently of the integrin-binding motif rgd. *Proc. Natl Acad. Sci. USA*, **95**, 5579–5583.

CLARK, R. A. F., DELLAPELLE, P., MANSEAU, E., LANIGAN, J. M., DVORAK, H. F. & COLVIN, R. B. (1982) Blood vessel fibronectin increases in conjunction with endothelial cell proliferation and capillary ingrowth during wound healing. *J. Invest. Dermatol.*, **79**, 269–276.

CLARK, R. A. F., DVORAK, H. F. & COLVIN, R. B. (1981) Fibronectin in delayed-type hypersensitivity skin reactions: associations with vessel permeability and endothelial cell activation. *J. Immunol.*, **126**, 787–793.

DAVIS, B. (1990) Reinforced random walk. *Prob. Th. Rel. Fields*, **84**, 203–229.

DAVIS, S., ALDRICH, T. H., JONES, P. F., ACHESON, A., COMPTON, D. L., JAIN, V., RYAN, T. E., BRUNO, J., RADZIEJEWSKI, C., MAISONPIERRE, P. C. & YANCOPOULOS, G. D. (1996) Isolation of angiopoietin-1, a ligand for the Tie2 receptor, by secretion-trap expression cloning. *Cell*, **87**, 1161–1169.

DENEKAMP, J. & HOBSON, B. (1982) Endothelial cell proliferation in experimental tumours. *Brit. J. Canc.*, **46**, 711–720.

FIRMANI, B., GUERRI, L. & PREZIOSI, L. (1999) Tumour/immune system competition with medically induced activation/deactivation. *Math. Models and Methods in Appl. Sci.*, **9**, 491–512.

FOLKMAN, J. (1971) Tumour angiogenesis: therapeutic implications. *N. Engl. J. Med.*, **285**, 1182–1186.

FOLKMAN, J. (1974) Tumour angiogenesis. *Adv. Canc. Res.*, **19**, 331–358.

FOLKMAN, J. & KLAGSBRUN, M. (1987) Angiogenic factors. *Sci.*, **235**, 442–447.

GATELY, S., TWARDOWSKI, P., STACK, M. S., CUNDIFF, D. L., GRELLA, D., CASTELLINO, F. J., ENGHILD, J., KWAAN, H. C., LEE, F., KRAMER, R. A., VOLPERT, O., BOUCK, N. & SOFF, G. A. (1997) The mechanism of cancer-mediated conversion of plasminogen to the angiogenesis inhibitor angiostatin. *Proc. Natl Acad. Sci. USA*, **94**, 10868–10872.

GATELY, S., TWARDOWSKI, P., STACK, M. S., PATRICK, M., BOGGIO, L., CUNDIFF, D. L., SCHNAPER, H. W., MADISON, L., VOLPERT, O., BOUCK, N., ENGHILD, J., KWAAN, H. C. & SOFF, G. A. (1996) Human prostate carcinoma cells express enzymatic activity that converts human plasminogen to the angiogenesis inhibitor, angiostatin. *Cancer Res.*, **56**, 4887–4890.

GIORDANO, F. J. & JOHNSON, R. S. (2001) Angiogenesis: the role of the microenvironment in flipping the switch. *Curr. Opin. Genet. Dev.*, **11**, 35–40.

HAN, Z. C. & LIU, Y. (1999) Angiogenesis: state of the art. *Int. J. Hematol.*, **70**, 68–82.

HANAHAN, D. & FOLKMAN, J. (1996) Patterns and emerging mechanisms of the angiogenic switch during tumourigenesis. *Cell*, **86**, 353–364.

HASHIZUME, H., BALUK, P., MORIKAWA, S., MCLEAN, J. W., THURSTON, G., ROBERGE, S., JAIN, R. K. & MCDONALD, D. M. (2000) Openings between defective endothelial cells explain tumour vessel leakiness. *Am. J. Pathol.*, **156**, 1363–1380.

HOLMES, M. J. & SLEEMAN, B. D. (2000) A mathematical model of tumour angiogenesis incorporating cellular traction and viscoelastic effects. *J. Theor. Biol.*, **202**, 95–112.

HUNT, T. K., KNIGHTON, D. R., THAKRAL, K. K., GOODSON, W. H. & ANDREWS, W. S. (1984) Studies on inflammation and wound healing: angiogenesis and collagen synthesis stimulated in vivo by resident and activated macrophages. *Surgery*, **96**, 48–54.

JONES, P. F. (1997) Tied up (or down?) with angiopoietins. *Angiogenesis*, **1**, 38–44.

KENDALL, R. L., RUTLEDGE, R. Z., MAO, X., TEBBEN, A. J., HUNGATE, R. W. & THOMAS, K. A. (1999) Vacular endothelial growth factor receptor kdr tyrosine kinase activity is increased by autophosphorylation of two activation loop tyrosine residues. *J. Biol. Chem.*, **274**, 6453–6460.

KIRSCH, M., SCHACKERT, G. & BLACK, P. M. (2000) Angiogenesis, metastasis and endogenous inhibition. *J. Neuro-Oncol.*, **50**, 173–180.

KLAGSBRUN, M. & D'AMORE, P. A. (1996) Vascular endothelial growth factor and its receptors. *Cytokine Growth Fact. Rev.*, **7**, 259–270.

LAI, W. H., CAMERON, P. H., WADA, I., DOHERTY, J. J., KAY, D. G., POSNER, B. I. & BERGERON, J. J. M. (1989) Ligand-mediated internalisation, recycling and downregulation of the epidermal growth factor receptor in vivo. *J. Cell Biol.*, **109**, 2741–2749.

LEUNG, D. W., CACHIANES, G., KUANG, W. J., GOEDDEL, D. V. & FERRARA, N. (1989) Vascular endothelial growth factor is a secreted angiogenic mitogen. *Sci.*, **246**, 1306–1309.

LEVINE, H. A., SLEEMAN, B. D. & NILSEN-HAMILTON, M. (2000) A mathematical model of the roles of pericytes and macrophages in the initiation of angiogensis: I. the role of protease inhibitors in preventing angiogenesis. *Math. Biosciences*, **168**, 77–115.

LEVINE, H. A., PAMUK, S., SLEEMAN, B. D. & NILSEN-HAMILTON, M. (2001a) A mathematical model of capillary formation and development in tumour angiogenesis: penetration into the stroma. *Bull. Math. Biol.*, **63**, 801–863.

LEVINE, H. A., SLEEMAN, B. D. & NILSEN-HAMILTON, M. (2001b) Mathematical modelling of the onset of capillary formation initiating angiogenesis. *J. Math. Biol.*, **42**, 195–238.

LEVINE, H. A., TUCKER, A. L. & NILSEN-HAMILTON, M. (2003) A mathematical model for the

role of cell signal transduction in the initiation and inhibition of angiogenesis. *Growth Factors*, **20**, 155–175.

LIOTTA, L. A., STEEG, P. S. & STETLER-STEVENSON, W. G. (1991) Cancer metastasis and angiogenesis: an imbalance of positive and negative regulation. *Cell*, **64**, 327–336.

LIU, W., AHMAD, S. A., REINMUTH, N., SHAHEEN, R. M., JUNG, Y. D., FAN, F. & ELLIS, L. M. (2000) Endothelial cell survival and apoptosis in the tumour vasculature. *Apoptosis*, **5**, 323–328.

LUCAS, R., HOLMGREN, L., GARCIA, I., JIMENEZ, B., MANDRIOTA, S. J., BORLAT, F., SIM, B. K. L., WU, Z., GRAU, G. E., SHING, Y., SOFF, G. A., BOUCK, N. & PEPPER, M. S. (1998) Multiple formas of angiostatin induce apoptosis in endothelial cells. *Blood*, **92**, 4730–4741.

MAISONPIERRE, P. C., SURI, C., JONES, P. F., BARTUNKOVA, S., WIEGAND, S. J., RADZIEJEWSKI, C., COMPTON, D., MCCLAIN, J., ALDRICH, T. H., PAPANDOPOULOS, N., DALY, T. J., DAVIS, S. & SATO, T. N. (1997) Angiopoietin-2, a natural antagonist for Tie2 that disrupts in vivo angiogenesis. *Sci.*, **277**, 55–60.

MOSER, T. L., STACK, M. S., WAHL, M. L. & PIZZO, S. V. (2002) The mechanism of action of angiostatin: can you teach an old dog new tricks?. *Thromb. Haemost.*, **87**, 394–401.

MURRAY, J. D. (1993) *Mathematical Biology* (2nd ed.). Berlin: Springer.

MUTHUKKARUPPAN, V. R. & AUERBACH, R. (1979) Angiogenesis in the mouse cornea. *Sci.*, **205**, 1416–1418.

MUTHUKKARUPPAN, V. R., KUBAI, L. & AUERBACH, R. (1982) Tumour-induced neovascularization in the mouse eye. *J. Natl Canc. Inst.*, **69**, 699–708.

NICOSIA, R. F., BONANNO, E. & SMITH, M. (1993) Fibronectin promotes the elongation of microvessels during angiogenesis in vitro. *J. Cell. Physiol.*, **154**, 654–661.

O'REILLY, M. S., HOLMGREN, L., SHING, Y., CHEN, C., ROSENTHAL, R. A., MOSES, M., LANE, W. S., CAO, Y., SAGE, E. H. & FOLKMAN, J. (1994) Angiostatin: a novel angiogenesis inhibitor that mediates the supression of metastases by a Lewis lung carcinoma. *Cell*, **79**, 315–328.

OTHMER, H. G. & STEVENS, A. (1997) Aggregation, blowup and collapse: the ABC's of taxis and reinforced random walks. *SIAM J. Appl. Math.*, **57**, 1044–1081.

PAPETTI, M. & HERMAN, I. M. (2002) Mechanisms of normal and tumour-derived angiogenesis. *Am. J. Physiol. Cell Physiol.*, **282**, C947–C970.

PAWELETZ, N. & KNEIRIM, M. (1989) Tumour related angiogenesis. *Crit. Rev. Oncol. Haematol.*, **9**, 197–242.

PEPPER, M. S. (1997) Manipulating angiogenesis. *Arterio. Thromb. Vasc. Biol.*, **17**, 605–619.

PEPPER, M. S. (2001) Extracellular proteolysis and angiogenesis. *Thromb. Haemost.*, **86**, 346–355.

PEPPER, M. S., BELIN, D., MONTESANO, R., ORCI, L. & VASSALLI, J. D. (1990) Transforming growth factor-β1 modulates basic fibroblast growth factor-induced proteolytic and angiogenic properties of endothelial cells in vitro. *J. Cell Biol.*, **111**, 743–755.

REYNOLDS, L. P., KILLILEA, S. D. & REDMER, D. A. (1992) Angiogenesis in the female reproductive cycle. *FASEB J.*, **6**, 886–892.

RISAU, V. (1997) Mechanisms of angiogenesis. *Nature*, **386**, 671–674.

SCHIRRMACHER, V. (1985) Cancer metastasis: experimental approaches, theoretical concepts and impacts for treatment strategies. *Adv. Canc. Res.*, **43**, 1–73.

SCHNELL, S. & MENDOZA, C. (1997) Closed form solution for time-dependent enzyme kinetics. *J. Theor. Biol.*, **187**, 207–212.

SEMENZA, G. L. (2000) HIF-1: Using two hands to flip the angiogenic switch. *Canc. Metast. Rev.*, **19**, 59–65.

SHOLLEY, M. M., FERGUSON, G. P., SEIBEL, H. R., MONTOUR, J. L. & WILSON, J. D. (1984)

Mechanisms of neovascularization. *Lab. Invest.*, **51**, 624–634.

SHWEIKI, D., ITIN, A., SOFFER, D. & KESHET, E. (1992) Vascular endothelial growth factor induced by hypoxia may mediate hypoxia-initiated angiogenesis. *Nature*, **359**, 843–845.

SLEEMAN, B. D. & WALLIS, I. P. (2002) Tumour induced angiogenesis as a reinforced random walk: modelling capillary network formation without endothelial cell proliferation. *J. Math. Comp. Modelling*, **36**, 339–358.

SOFF, G. A. (2000) Angiostatin and angiostatin-related proteins. *Canc. Metastasis Rev.*, **19**, 97–107.

STACK, M. S., GATELY, S., BAFETTI, L. M., ENGHILD, J. J. & SOFF, G. A. (1999) Angiostatin inhibits endothelial and melanoma cellular invasion by blocking matrix-enhanced plasminogen activation. *Biochem. J.*, **340**, 77–84.

STOKES, C. L. & LAUFFENBURGER, D. A. (1991) Analysis of the roles of microvessel endothelial cell random motility and chemotaxis in angiogenesis. *J. Theor. Biol.*, **152**, 377–403.

TURNER, S. & SHERRATT, J. A. (2002) Intercellular adhesion and cancer invasion: a discrete simulation using the extended potts model. *J. Theor. Biol.*, **216**, 85–100.

UNEMORI, E. N., FERRARA, N., BAUER, E. A. & AMENTO, E. P. (1992) Vascular endothelial growth factor induces interstital collagenase expression in human endothelial cells. *J. Cell. Physiol.*, **153**, 557–562.

VAJKOCZY, P., FARHADI, M., GAUMANN, A., HEIDENREICH, R., ERBER, R., WUNDER, A., TONN, J. C., MENGER, M. D. & BREIER, G. (2002) Microtumour growth initiates angiogenic sprouting with simultaneous expression of VEGF, VEGF receptor-2 and angiopoietin-2. *J. Clin. Invest.*, **109**, 777–785.

VERNON, R. B. & SAGE, E. H. (1999) A novel quantitative model for study of endothelial cell migration and sprout formation within three-dimensional collagen matrices. *Microvasc. Res.*, **57**, 118–133.

YANCOPOULOS, G. D., DAVIS, S., GALE, N. W., RUDGE, J. S., WIEGAND, S. J. & HOLASH, J. (2000) Vascular-specific growth factors and blood vessel formation. *Nature*, **407**, 242–249.

Appendix A. Substrate numerics

Replacing the derivatives in (53) by finite difference approximations (using Crank–Nicholson finite difference for spatial derivatives),

$$\frac{V(x,y,t+k)-V(x,y,t)}{k} = K_{21}\frac{1}{2h^2}\left(\Phi(x,y,t+k) - 4V(x,y,t+k) + \Phi(x,y,t) \right.$$
$$\left. -4V(x,y,t)\right) - K_1\frac{V(x,y,t)\,P(x,y,t)}{1+V(x,y,t)},$$

where $\Phi(x,y,t) = V(x-h,y,t) + V(x+h,y,t) + V(x,y-h,t) + V(x,y+h,t)$.

This leads to the iterative scheme

$$V(x,y,t+k) = \frac{k}{h^2+2K_{21}k}\left(\frac{K_{21}}{2}\left(\Phi(x,y,t+k) + \Phi(x,y,t)\right)\right.$$
$$\left. + \left(\frac{h^2}{k} - 2K_{21} - \frac{h^2K_1P(x,y,t)}{1+V(x,y,t)}\right)V(x,y,t)\right).$$

The BC at the capillary (61) becomes

$$0 = -K_{33}\frac{V(x,h,t) - V(x,0,t)}{h} + V(x,0,t) - v(x,t)$$
$$\Rightarrow V(x,0,t) = \frac{1}{K_{33}+h}\left(K_{33}V(x,h,t) + hv(x,t)\right).$$

The BC at the tumour (65) becomes

$$\frac{V(x,l/L,t) - V(x,l/L-h,t)}{h} = K_{35}\left(1-\cos(2\pi x)\right)^{m_0}$$
$$\Rightarrow V(x,l/L,t) = V(x,l/L-h,t) + K_{35}h\left(1-\cos(2\pi x)\right)^{m_0}.$$

and the BCs at $x = 0, 1$ (70) become

$$V(0,y,t) = V(h,y,t)$$
$$V(1,y,t) = V(1-h,y,t).$$

The fibronectin equation (55) gives the iterative scheme

$$F(x,y,t+k) = \frac{k}{h^2+2K_{22}k}$$
$$\left(\frac{K_{22}}{2}\left(\Gamma(x,y,t+k) + \Gamma(x,y,t)\right) + U(x,y,t)\,F(x,y,t)\right),$$

where $\Gamma(x,y,t) = F(x-h,y,t) + F(x+h,y,t) + F(x,y-h,t) + F(x,y+h,t)$ and $U(x,y,t) = \frac{h^2}{k} - 2K_{22} + K_{23}h^2\left(1-F(x,y,t)\right) - \frac{K_5h^2C_A(x,y,t)}{1+K_6F(x,y,t)}$.

The BCs (62), (66) and (71) become

$$F(x,0,t) = F(x,h,t)$$
$$F(x,l/L,t) = F(x,l/L-h,t)$$
$$F(0,y,t) = F(h,y,t)$$
$$F(1,y,t) = F(1-h,y,t).$$

The angiostatin equation (56) gives

$$A(x,y,t+k) = \frac{k}{h^2+2K_{24}k}\left(\frac{K_{24}}{2}\left(\Pi(x,y,t+k) + \Pi(x,y,t)\right)\right.$$
$$\left. + h^2K_7H(t-K_8)\left(1-F(x,y,t)\right) + W(x,y,t)\,A(x,y,t)\right),$$

where $\Pi(x,y,t) = A(x-h,y,t) + A(x+h,y,t) + A(x,y-h,t) + A(x,y+h,t)$ and $W(x,y,t) = \frac{h^2}{k} - 2K_{24} - h^2K_9$.

The BCs (63), (67) and (72) become

$$A(x,0,t) = \frac{1}{K_{34}+h}\left(K_{34}A(x,h,t) + ha(x,t)\right)$$
$$A(x,l/L,t) = A(x,l/L-h,t)$$
$$A(0,y,t) = A(h,y,t)$$
$$A(1,y,t) = A(1-h,y,t).$$

Note that in the computations, the *density* at mesh point is calculated as being proportional to the *number* of cells at that point, with the constant of proportionality chosen so that the mean initial density in the capillary is 1. Thus if p_i and N_i are respectively the cell density and the number of cells at point i in the capillary then $p_i = kN_i$ and we choose k such that

$$\frac{1}{n}\sum_{i=1}^{n} p_i \equiv \frac{kN}{n} = 1$$

$$k = \frac{n}{N}$$

where n is the number of grid points and $N = \Sigma_{i=1}^{n} N_i$ is the total number of cells.

Similarly, in the ECM we set $p_{ij} = KN_{ij}$. Note that the total mass in the capillary is 1 and so the total mass of N cells in the ECM should also be 1. We must therefore have

$$\frac{1}{n^2}\sum_{i=1}^{n}\sum_{j=1}^{n} p_{ij} \equiv \frac{KN}{n^2} = 1$$

$$K = \frac{n^2}{N}.$$

This unusual relationship between the scaling constant in the capillary and that in the ECM arises because of the coupling of a one-dimensional and a two-dimensional system via the transmission conditions, (28), (30)–(33).

Appendix B. Parameter values

The following parameter values were used in the simulations:
Length of domain: $L = 0{\cdot}05$ mm
EC diffusion coefficient: $D_p = D_P = 3{\cdot}6 \times 10^{-6}$ mm^2 h^{-1}
VEGF diffusion coefficient: $D_V = 3{\cdot}6 \times 10^{-5}$ mm^2 h^{-1}
Fibronectin diffusion coefficient: $D_F = 3{\cdot}6 \times 10^{-10}$ mm^2 h^{-1}
Angiostatin diffusion coefficient: $D_A = 6{\cdot}5 \times 10^{-5}$ mm^2 h^{-1}
Kinetic parameters for VEGF: $\lambda_1 = 74{\cdot}769231$ h^{-1}, $\nu_1 = 0{\cdot}007692308$ μM^{-1}
Kinetic parameters for fibronectin: $\lambda_3 = 19{\cdot}277108$ μM^{-1} h^{-1}, $\nu_3 = 1{\cdot}2048193$ μM^{-1}
Protease inhibitor equilibrium constant: $\nu_e = 1\mu$M^{-1}
Protease decay rate: $\mu = 4{\cdot}56$ h^{-1}
Fibronectin production times: $T_f = T_F = 18$ h
Angiostatin decay time: $T_a = 1$ h
Proliferation rates: $Q = 8 \times 10^{-4}$ h^{-1}, $A = 44{\cdot}13$ μM^{-1}, $\lambda_0 = 1{\cdot}1 \times 10^{-9}$ μM^{-2}, $m_1 = 2$
Death rate: $\mu_1 = 7{\cdot}142857 \times 10^{-5}$ h^{-1}
Threshold values: $f_0 = 6 \times 10^{-3}$ μM, $T_{iv} = 4{\cdot}5$ h
VEGF transmission rates: $B_1 = 1{\cdot}0$ h^{-1}, $\psi = 2$ mm h^{-1}
Angiostatin transmission rate: $\psi' = 2$ mm h^{-1}
VEGF source term constants: $v_0 = 0{\cdot}04$ μM mm^2 h^{-1}, $\sigma = 1{\cdot}514705513 \times 10^{-3}$
Angiostatin source term constant: $A_r = 1700$ μM h^{-1}

Initial EC density: $p_0 = 10^{-5}\ \mu$M
Initial fibronectin level: $f_0 = 10^{-2}\ \mu$M
Number of receptors per cell: $\delta_e = 10^5$
Protease transition probability parameters: $\alpha_1 = 0{\cdot}1\ \mu$M, $\alpha_2 = 1{\cdot}0\ \mu$M, $\alpha_3 = 0{\cdot}1\ \mu$M, $\alpha_4 = 1{\cdot}0\ \mu$M
Fibronectin transition probability parameters: $\beta_1 = 1{\cdot}0\ \mu$M, $\beta_2 = 0{\cdot}1\ \mu$M, $\beta_3 = 1{\cdot}0\ \mu$M, $\beta_4 = 0{\cdot}5\ \mu$M
VEGF transition probability parameters: $\delta_1 = 0{\cdot}1\ \mu$M, $\delta_2 = 1{\cdot}0\ \mu$M, $\delta_3 = 0{\cdot}1\ \mu$M, $\delta_4 = 1{\cdot}0\ \mu$M
Transition probability exponents: $\gamma_1 = 100$, $\gamma_2 = 100$, $\gamma_3 = 40$, $\gamma_4 = 50$, $\gamma_5 = 37{\cdot}5$, $\gamma_6 = 20$.

Many of these values are taken from Levine *et al.* (2001a). Here we discuss the values that are particular to this model.

Diffusion coefficients. The substrate diffusion coefficients, D_V, D_F and D_A were taken to be a factor of 100 smaller than in Levine *et al.* (2001a) so that the chemotactic and haptotactic gradients that the EC detect are not destroyed.

Proliferation rate. Levine *et al.* (2001a) used a proliferation rate, Q, which depended on the curvature of the capillary tips. In a discrete model such as the one presented here, we are concerned with individual cells and so it does not make sense to talk of vessel curvature. We therefore use a constant value of Q within the range of values used in the curvature-dependent case.

VEGF and angiostatin source terms. Here we used a smaller value than Levine *et al.* (2001a) for the VEGF source term constant and a larger value for the angiostatin source term constant. The effects of changing the values of these parameters are discussed in Section 4.

VEGF transition probability parameters. Levine *et al.* (2001a) used a transition probability function of the form $\tau_1(c_a)\,\tau_2(f)$. Here we have also included a term $\tau_3(v)$ and we have used the same parameters in the VEGF transition function, τ_3, as in the protease transition function, τ_1.

Transition probability exponents. We have used larger values for the exponents in the transition probability function than Levine *et al.* (2001a) in order to elicit an adequate chemotactic response from the EC.